Master Thesis

Silvia Briones Herranz

Modelling the ventilation-perfusion mismatch of the cardiopulmonary system in Matlab Simscape

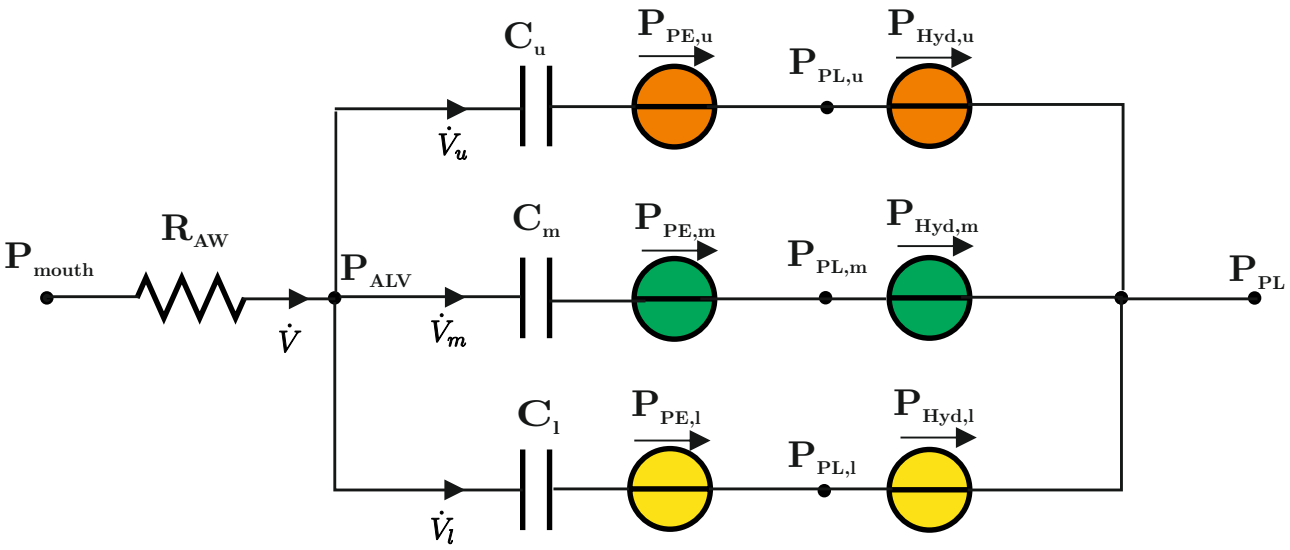

LEHRSTUHL FÜR MEDIZINISCHE INFORMATIONSTECHNIK
Univ.-Prof. Dr.-Ing. Dr. med. Steffen Leonhardt
Supervising Tutor: Dipl.-Ing. Ngo Chuong
Date: October 25, 2015

Acknowledgments

First and foremost, I offer my sincerest gratitud to MedIT, its director, Univ.-Prof. Dr.-Ing. Dr. med. Steffen Leonhardt, and its staff for this great opportunity to develop my master project in this Institute.
In particular, I would like to express my deepest gratitude to my supervisor, Dipl.-Ing. Chuong Ngo who has supported me throughout my thesis with his patience and assistance.
I would like to extend my thank to my friends for their motivation and support.
Finally, I would like to express my gratefulness to my parents Maria Teresa and Juan Carlos, my sister Patricia and my brother Alberto for their encouragement, love and support through the duration of my studies.

Declaration

I hereby declarate that this thesis entitled “Modelling the ventilation-perfusion mismatch of the cardiopulmonary system in Matlab Simscape” is the result of my own work and that, to the best of my knowledge and belief, it contains no material previously published or written.

Place, Date

Signature

Abstract

A novel model of perfusion distribution in the lung and a novel model of ventilation distribution are developed in this thesis. Both models are focused on the pressure distribution along the thorax due to the gravitation.

The lung is divided into three zones: upper zone, middle zone and lower zone. Blood flow increses with the distance from the top of the lung. The upper zone is characterized by a complete collapse of the pulmonary capillary vasculature, thus there is no flow in this zone. The second zone have a "Waterfall effect", the blood flow is determinated by the difference between the pulmonary artery and alveolar pressures. In the lower zone, the flow is purely driven by the difference between the pulmonary artery pressure and the pulmonary vein pressure. In ventilation, the upper lobe of the lung are more expanded than the middle and lower lobes at resting position. Consequently, ventilation during spontaneous breathing was found nonuniform with more air entering the lower lobes than the middle and upper lobes.

As a result, a complete model of perfusion and ventilation in the lung is created and the results obtained in both models are in good agreement with the litetature. Both models are implemented in the object-oriented modeling and simulation module Matlab Simscape.

Contents

List of Figures

List of Tables

Nomenclature

Acronyms

EN	Erythrocyte
EN	Capillary Endothelium
EP	Alveolar Epithelium
FRC	Expiratory Reserve Volume
FRC	Functional Residual Capacity
IRV	Inspiratory Reserve Volume
TLC	Total Lung Capacity
FRC	Vital Capacity

Physical Quantities

b	Elastic Constant	cm^{-1}
C	Compliance	$\mathrm{L\,cmH_2O^{-1}}$
d	Distance	cm
k	Elastic Constant	$\mathrm{cmH_2O^{-1}}$
L	Lung Distance	cm
m	Constant	-
P	Pressure	$\mathrm{cmH_2O}$
q	Blood Flow	$\mathrm{L\,s^{-1}}$
R	Resistance	$\mathrm{cmH_2O\,s\,L^{-1}}$
t	Time	s
V	Volume	L
$\dot{\mathrm{V}}$	Air Flow	$\mathrm{L\,s^{-1}}$

Subscripts

0	Initial Volume
a	Arterial
A	Alveolar (Ventilation)
ALV	Alveolar (Pressure)
AW	Airway
c	Capillary
cp	Capillary bed
cw	Chest Wall
D	Dead Space
E	Transmural
Hdy	Hydrostatic
l	Lower Zone - Lower Lobe
m	Middle Zone - Middle Lobe
o	Maximal pulmonary volume
pa	Pulmonary Artery
PE	Extended Pleural
PL	Pleural
pv	Pulmonary Vein
T	Tidal (Volume)
T	Total (Capacity)
TP	Transpulmonary
u	Upper Zone - Upper Lobe
v	Venous

1 Introduction

The ventilation-perfusion ratio represents the relationship between the amount of air that receive the alveoli (alveolar ventilation, V) and the amount of blood that is driven from the heart to the lung (perfusion, Q). When a problem occurs in the lungs related to the ventilation or perfusion or both, this ratio is not evenly matched. This V/Q mismatch (or inequality) is found typically in the chronic obstructive pulmonary disease (COPD), which affects more than 200 million people and is the fourth leading cause of death in the world.[FIR]

Moreover, the Forum of International Respiratory Societies (FIRS) has revealed the alarming data of over 4 million people death annually due to lung disease and this death rate continue rising [FIR].

Although the overall ventilation-perfusion ratio is matched in a normal person, the effect of the gravity in the lung makes that we have different ventilation-perfusion rates along the lung. In this thesis we develop and implement two physiological models: one related to the perfusion distribution throughout the lung in upright position and the other related to the ventilation. With these models we represent how the gravity affects in both distributions and therefore, in the ventilation-perfusion ratio. In addition, these lung models pretend to accomplish with their simulations a totally and exactly behavior of the lungs, that it can be used by the doctor to determinate the correct diagnostics.

1.1 Ventilation-Perfusion Modelling -State of the Art

Several models have been developed to describe different aspects of the ventilation or perfusion in the lung with different perspectives and at different levels of detail. However, none had developed a physiological model that joins the pulmonary ventilation model and the pulmonary perfusion model with respect the effect of the gravity.

In the literature [KKA$^+$10], [BT06], [Gle08] some gas-exchange models use continuous ventilation and perfusion in order to describe pulmonary gas-exchange and gas mixing in the lungs. Although these models describe the physiological processes in an intuitive way, the ventilation and perfusion are not continuous, they are affected by different parameters i.e. the effect of tissue elasticity, the effect of hydrostatic pressure, the effect of intrapleural pressure, the effect of alveolar pressure.

Other models exist which use non-physiological analogies such as springs or dashpots for the lung but they are unable to improve our understanding of the local behavior of the respiratory system.

The literature provides mathematical models focused exclusively on pulmonary circulation [MSKA09] as well as a part of the implementation in the circulatory system [Hel04]. There are also models focused on airway and lungs mechanics [LWHR82], [OMB+56],[PSME72] and gas exchange [Hla72],[LC73]. However, the variation on the vertical distance along the lung is not contemplated in these models. Liu et al. [LNCJ+98] were the first authors who combine ventilation, gas-exchange and perfusion in a nonlinear model of the normal human lungs. However, the model that they described does not present the local behavior of ventilation and perfusion in the lungs, and still consider the lungs as a lumped single compartment. On the other hand, Mogense el al. [Mog11] presented a total mathematical model of the respiratory system. His model is subdivided in four parts: the ventilation, perfusion, gas exchange and blood. He considers different physiological components such as the capillary geometry, the blood viscosity and the geometric model of the alveoli. However, the gravity is not contemplated ventilation model whereas it is in the perfusion one. Nevertheless this model simulates a healthy human in the supine posture during mechanical ventilation. In this work we develop a model based in upright posture whose behavior is different.

Moreover, Otis et al. [OMB+56] apphoached with a mechanical model repesented in Figure 1.1(a) the distribution of pulmonary ventilation, but the effect of the gravity is not considered. On the other hand, Pedley et al.[PSME72] Yeh and Schum [YS80] developed a mathemathical model where the lung is divided into two lobes (see Figure 1.1(b)) and five lobes respectively. In both cases, the vertical gradient of transpulmonary pressure is contemplated.

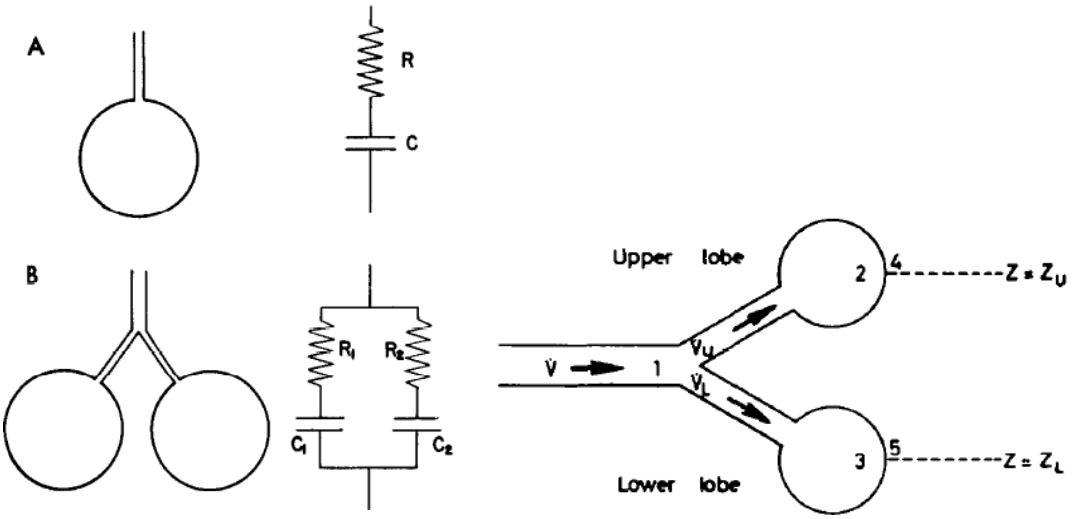

(a) Model proposed by Otis et al.[OMB+56]

(b) Two-compartiment model of the lung by Pedley et al.[PSME72]

Figure 1.1: Models proposed of the lung

1.2 Motivation and Aims of this Research

The effect of gravity in the lung makes that we have different ventilation-perfusion rates along the lung. A model which represents the distribution of perfusion and ventilation along the vertical axis of the lung as well as the ventilation-perfusion ratio, is useful for doctors to locate the affected zone and to achieve the correct diagnostic and therapy.

The aim of this study is develop and implement two physiological models in order to describe the distribution of ventilation and perfusion in the lungs of a healthy human in upright position by mean of Matlab Simscape. In these models we focus on the effect of gravity using the three zones of the lung described by Dr. John B. West [Wes12] in a way that with these models we can clarify how the gravity may affect the distribution of ventilation and perfusion. Once both models would be developed and implemented, the third goal is determine the ventilation-perfusion ratio at different levels of the lung. Consequently, first of all it is necessary to understand the behavior of the healthy lungs and then develop the models of this behavior.

1.3 Organization of the thesis

The thesis is organized by the following chapters where a brief description of its contents is also included:

The introduction, the motivation, aims and organitation of the thesis is presented in the **Chapter 1**. Basic knowledge about the physiology of the lung, analogous quantities in mechanical and electrical systems, and a brief understanding of the pulmonary circulation and ventilation are exposed in the **Chapter 2**. A brief description of the tool used for the implementation of the models is presented in the **Chapter 3**. The **Chapter 4** contains a mathemathical development of the distribution of perfusion along the lung as well as the development and implementation of the eletrical model equivalent to this distribution. The **Chapter 5** includes a mathemathical development of the distribution of ventilation along the lung and the eletrical model equivalent associated with this distribution. The simulations of both models and the corresponding explications are provides in **Chapter 6**. **Chapter 7** concludes this master thesis where the future works and the overall conclusions are exposed.

2 Physiology of the Lung

The lungs represented in Fig.2.1, are a pair of large and spongy essential organs in the respiration. Although we relate the respiration to repeated inhaling and exhaling of air and its respective movements of the thorax, it is a complex process with the following goals:

- Providing oxygen to the tissues, in order to get enough energy to realize metabolic cellular functions.
- Expelling carbon dioxide through the gas-exchange.

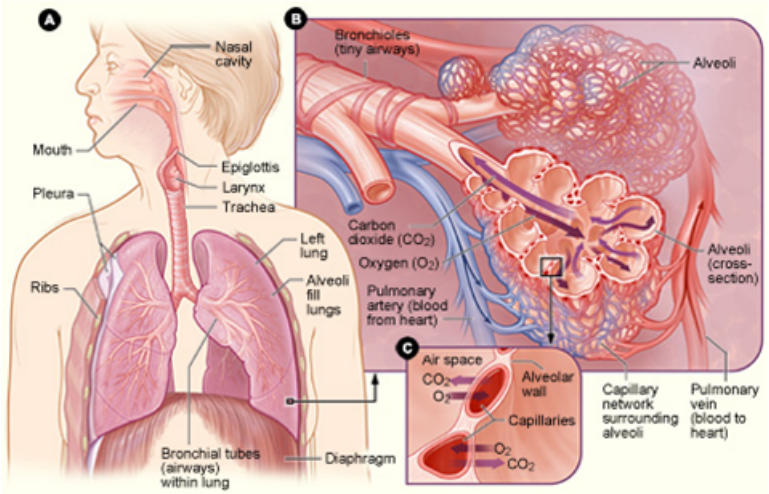

Figure 2.1: The respiratory system (A) the upper and lower airway divisions (B) Alveoli (C) Gas-exchange. Adapted from [Res].

We can distinguish three parts of the respiration process: **1)** the ventilation via airways in the lungs, the movement of air between the atmosphere and the alveoli **2)** the pulmonary circulation, to move to and from the lung and finally, **3)** gas exchange based on the transport and distribution of oxygen (O_2) and carbon dioxide (CO_2) in the respiratory system. All of them are essential to achieve oxygenate all the cells of our body, required to live.

2.1 Anatomy of the Respiratory System

When the gas moves in and out of the lungs by means of the conduction zone, the lungs are expanded and contracted, respectively. We can divide the conduction zone in two parts principally.

The first one, **upper airway division**, which is in contact with the environment, is formed by the mouth, nasal cavity, pharynx and larynx. **The lower airway** division extends from the trachea to the terminal bronchioles; the trachea divides into right and left primary bronchi. bronchi is divided into the secondary bronchi within each lung. This division into segmental bronchi occurs successively within the lung until 16 generations [Wes12] where the bronchi are becoming narrower each time as far as the terminal bronchioles. The terminal bronchioles enclose alveolar ducts which drive air to a network of air sacs called alveoli (see Fig. 2.1).

When a person takes in a breath of air, the air runs through the nasal cavity and mouth to the larynx. In this process the atmospheric air is warmed to body temperature and is humidified. The ciliated mucous membranes filter and retain particles of the incoming air to keep it clean. Then, the clean air flows through the trachea where is separated into the branching tubes until the alveoli where the gas-exchange takes place.

2.2 Ventilation

Ventilation is the movement of air into and out of the lungs by mean of inhalation and exhalation. It necessary a positive difference of pressure between the environment (atmospheric pressure, 760 mmHg) to the alveoli, to produce the air moves into the alveoli (the intra-alveolar pressure exceed the atmospheric pressure). On the other hand, a positive difference of pressure between the alveoli and the environment produce the air moves out of the alveoli.

2.2.1 Mechanics of pulmonary ventilation

There are diverse muscles that cause the expansion and compression of the lungs in the inspiration and expiration, respectively. Fig.2.2 represents the changes in lung volume and pressures during normal breathing.

INSPIRATION

With the contraction of the diaphragm, the volume of the thoracic cavity increases and the air is drove into the lungs. During more forceful inspirations the muscles between the ribs, external intercostals, and other muscles are necessaries to elevate the rib cage and to expand the lungs. These muscles are classified as muscles of inspiration. As a result of thorax expansion due to the contraction of these muscles, the pressure inside the pleural cavity, intrapleural pressure, decrease. It causes the lungs to increase in size and thus, the pressure inside the lung (intrapulmonary pressure) also decrease with respect to the barometric pressure. This pressure difference causes the air to be driven into

the alveoli. Moreover, the transpulmonary pressure, which is the difference between the intrapulmonary pressure and intrapleural pressure, is also reduced [GH12][Wes12].

It should be pointed out that the pleural pressure is always negative, although it varies according to the process of respiration. This negative force outside the lungs is required to keep the lungs expanded, as their elastic recoil tends to collapse them.

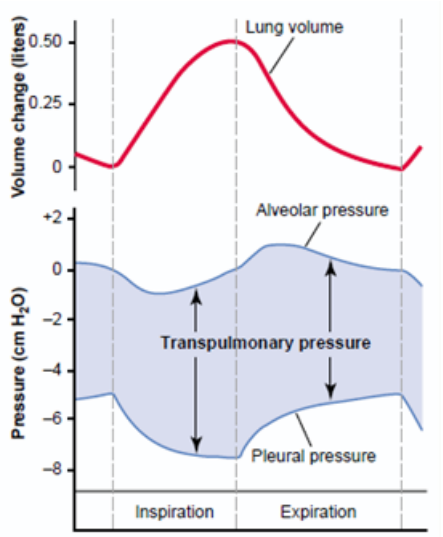

Figure 2.2: Changes in the lung volume, alveolar pressure, pleural pressure, and transpulmonary pressure during normal breathing. Adapted from [GH12].

EXPIRATION

The expiration begins when the diaphragm relaxes, whereas the chest wall and abdominal structures compress the lungs to eject the air inside of them. These movements allow a reduction in the thoracic volume and a momentarily increment of the pressure inside the pleural cavity which causes a reduction in the alveolar volume and a rise in the intrapulmonarly or alveolar pressure. As a conclusion, the air flows out the lungs owing to this difference of pressure [Wes12][GH12].

2.2.2 Lung Volumes and Capacities

A distribution of the statics volumes throughout the lung is presented [Wes12]. In Fig.2.3 a driagram of the different volumes in the lung is represented.

With each normal inspiration, about 500 milliliters of air enters in the conducting zone (tidal volume) to reach the alveoli [GH12]. This among of gas is supposed to be expelled during the expiration. As there are no alveoli in the first part of the conduction zone, no gas-exchange of oxygen and carbon dioxide is realized. Thhis zone is called anatomic dead

space. About 150 milliliters of air are wasted in this part; it supposes about 30% of the tidal ventilation [GH12][Wes12].

When a person inhale more forceful, maximal inspiration, an additional volume of air can be inspired over the normal tidal volume, it is called inspiratory reserve volume (IRV) and is equal to 3000 milliliters normally. In the same way the expiratory reserve volume (ERV) is the extra volume of air that can be exhaled by a subject while forces his lungs as much as possible after the end of a normal expiration; this is usually equal to 1100 milliliters. During exercise, tidal volume is increased because of the increased dependence on inspiration reserve volume and expiration reserve volume [GH12][Wes12].

There is certain among of gas that remains in the lungs after a maximal expiration, it is the residual lung volume and its mean is approximately 1200 milliliters.

Normally, the spirometry is used to measure these volume movements of air into and out of the lung that have been presented.

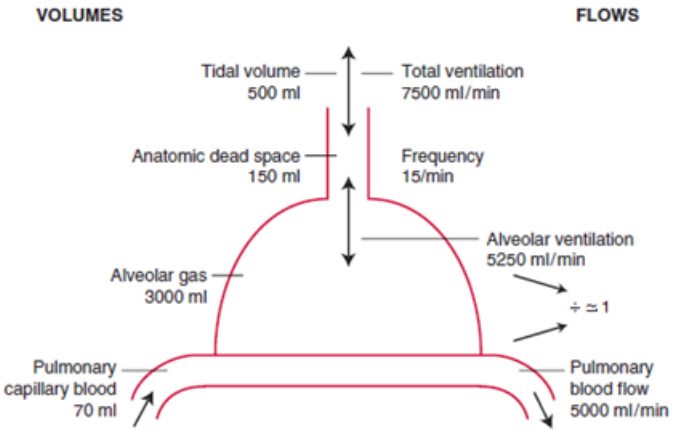

Figure 2.3: Diagram of a lung showing typical volumes and flows. Adapted from [Wes12]

To clarify the values of total ventilation per minute, it is necessary to consider the tidal volume, about 500 ml, and the breathing frequency per minute; it is around 15 per minute, as result (500 x 15) =7500 ml/min. Moreover, the alveolar ventilation is equal to the volume difference between tidal ventilation and anatomic dead space, and multiplied with the breathing frequency, as result (500-100) x 15 = 5250 ml/min.

The important pulmonary capacities (see Fig.2.4) can be described as follows [GH12][Wes12].

- 1) The inspiratory capacity is equals to the tidal volume plus the inspiratory reverse volume. It is about 3500 milliliters and this is the maximal amount of air a subject can inhaled from the end of a normal exhalation.

- 2) The amount of air that remains in the lungs after a normal expiration, about 2300 milliliters, is known as the functional residual capacity and it is equal to the expiratory reverse volume plus the residual volume.

- 3) When tidal volume is maximal, this means that is enclosed the tidal volume plus the inspiratory reserve volume plus the expiratory reverse volume, it is called vital capacity (VC) and it represents the maximum volume of air exhaled after a maximal expiration. It is approximately about 4600 milliliters.

- 4) Together, the vital capacity and the residual volume form the total lung capacity. It is approximately 5800 milliliters and it corresponds to the maximum volume of the lungs during a grater enforce.

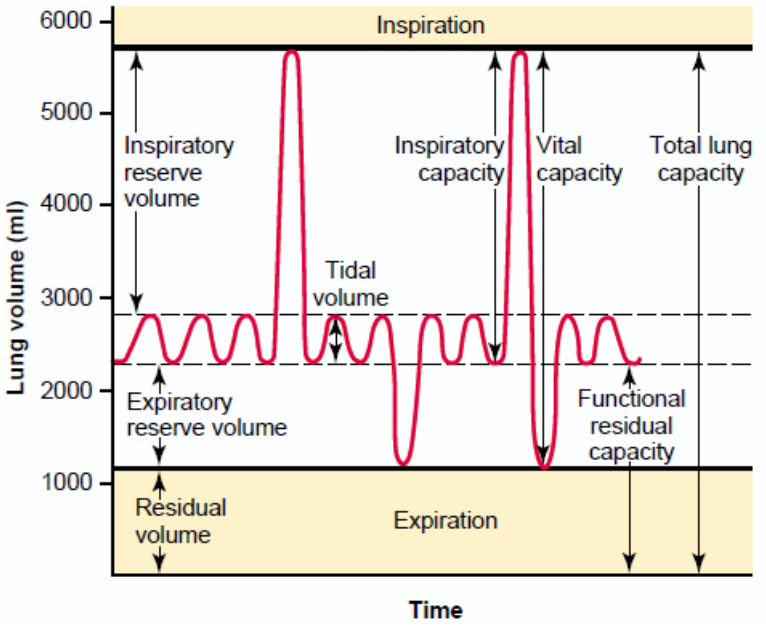

Figure 2.4: Diagram showing the capacities and volumes of the lung. Adapted from [GH12]

All pulmonary volumes and capacities are correlated to body size and gender. Normally it used to be less in healthy women than in healthy men, about 20% to 25%.

2.2.3 Regional differences in ventilation

By mean of diverse studies ,such as those made with differencial lobar bronchospirometry realized by [MY56] or more recently with radioactive gas realized by West and Dollery [WD60] and Milic-Emili et al. [MEHD+66], it have been demostrated that all regions in the lungs have different ventilation. In Fig.2.5 is represented this distribution:

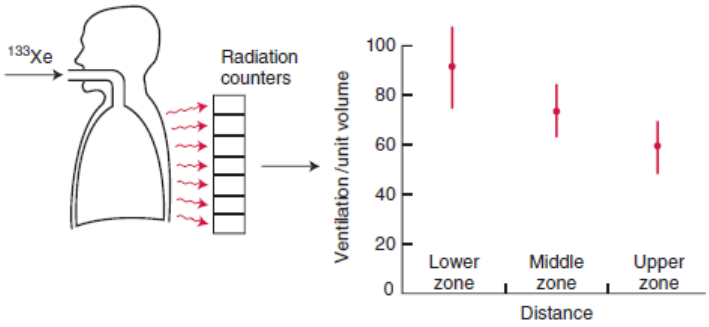

Figure 2.5: Measurement of regional differences in ventilation with radioactive xenon. Adapted from [Wes12].

As is shown in Fig.2.5, the ventilation in the lower zone of the lung is greater than the upper zone. This is because of the intrapleural pressure is less negative at the bottom than the apex of the lung, which is caused by the weight of the lung. As a consecuence, in resting state the basal lung is relatively compressed but it is expanded more than the apex when we inhale. In Fig.2.6 is represented this changes of intrapleural pressure.

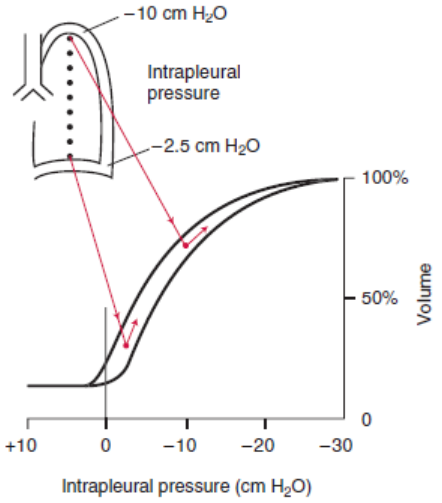

Figure 2.6: Intrapleural pressure along the lung. Adapted from [Wes12].

2.3 Pulmonary Circulation

Fig.2.7 presents a schematic structure of the pulmonary circulation. Blood is delivered from the right ventricle to the pulmonary artery. The artery consists of branching structures forming a tree called arterioles. These arterioles are divided in thin vessels called capillaries. Then the oxygenated blood converge into larger pulmonary veins, and finally the blood leave the lung to the left atrium.

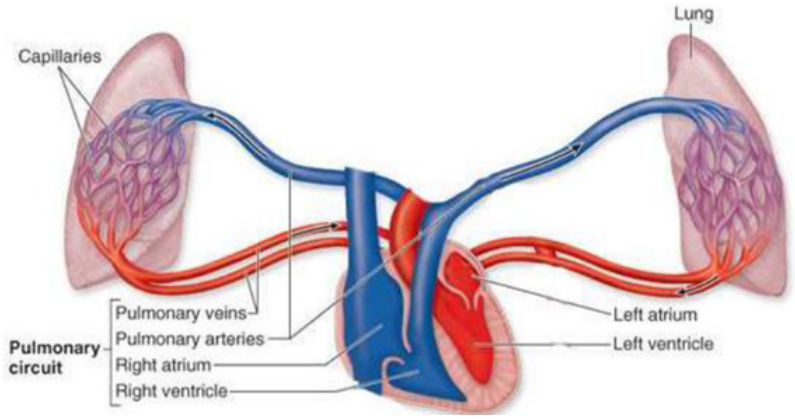

Figure 2.7: The pulmonary circulation. Blue indicates deoxygenated blood and red oxygenated blood. Adapted from [PC]

The capillaries consist of a network of thin vessels surrounding alveoli (Fig.2.1 (B-C)). Each capillary is constituted by two membranes, and in the space between these membranes the fluid flows. The blood-gas barrier is formed by the alveolar epithelium (EP), an interstitium, the capillary endothelium (EN), and plasma [Wes12], see Fig.2.8. The gas of the alveolus (A) goes to the interior of the erythrocyte (EC). This blood-gas barrier could be extremely thin in some areas, less than $0.3\mu m$.

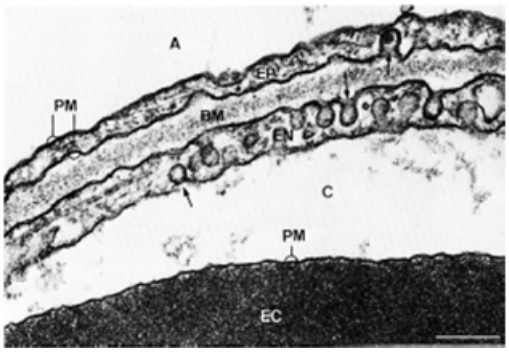

Figure 2.8: Very high-power electron micrograph showing the pulmonary blood-gas barrier. Adapted from [WD13]

The transport of oxygen and carbon dioxide across the blood-gas barrier occurs by passive diffusion, that is, the gasses are always characterized to move from regions with high partial

pressure to another with low partial pressure, as long as it is physically possible [Wes12].

2.3.1 Low-resistance pulmonary circulation system

The pulmonary circulation is characterized by low resistance and high compliance. Pulmonary vascular resistance is extremely low, more or less about one-tenth that of systemic vascular resistance [Wes12]. It is due to of the immense number of small vessels that are dilated. This Pulmonary vascular resistance is equal to the difference of pressure (ΔP) divided by blood flow (Q)

About 0.25 sec is the time that, a red blood cell remains in the alveolar capillary network where it passes through of two or three alveoli. This period of time is sufficient to equilibrate oxygen and carbon dioxide between alveolar gas and capillary blood. The low resistance is necessary to allow the same amount of blood the heart pumping through the circulatory system within a short period of time, goes to the pulmonary circulatory system.

In addition, an important characteristic of the pulmonary circulation is the capacity to decrease resistance when an increase in the pulmonary arterial pressure (Ppa) is produced. When we realize exercise, an increase in the cardiac output is produced and thus, a rise of pulmonary arterial and venous pressure. With this property it accomplishes to reduce the physiological stress loaded on the thin blood-gas barrier [Wes12]. These responses are completely different from those in the systemic circulation, where an increase in pressure produce increases in vascular resistance.

There are two mechanisms that are responsible in the low-resistance:

- The process of opening capillaries (previously closed) is the first mechanism for the fall in pulmonary vascular resistance when cardiac output rises.

- The second one is the capillary distension (once the capillaries are open), which occurs because the pulmonary capillaries are excessively thin and with high compliance (C).

The lung volume, represented in Subsec.2.2.2 also affects the pulmonary vascular resistance due to the structural support that the pulmonary capillaries have which can be easily expanded or collapsed depending on the pressure surrounding them. The change in the vessels diameter is due to the difference of pressure outside the capillary and inside the capillary, this difference is known as transmural pressure. We can classified the pulmonary vessels in two types, extra-alveolar vessels which are subjected to pleural pressure and it include pulmonary arteries and veins, and alveolar vessels which include precapillaries, capillaries and postcapillaries, and in this case are subjected to alveolar pressure[Wes12][GH12]

2.3.2 Low-pressure pulmonary circulation system

Moreover, the pulmonary arteries, the pulmonary veins and in conclusion, the pulmonary vasculature is also low-pressure, it is represented in Fig.2.9.

A cardiac cycle is divided into two phases: **diastole** and **systole**. Diastole represents the period of time when the heart venticles are relaxing whereas systole represents the time during the left and right ventricles eject blood into the aorta and pulmonary artery respectively. The pulmonary arterial pressure fluctuate between 25 mmHg (systole) and 8 mmHg (diastolie) [GH12][Wes12]. Therefore, the average in the main pulmonary arterial is about 15 mmHg. By contrast, the aorta have an average about 100 mmHg, it is about six times higher than in the pulmonary artery.

The pressure within the pulmonary capillaries is ambiguous because of hydrostatics effects, which produce variations in the capillaries throughout the lung. However, using the technique "isogravimetric" according to West [Wes12] it is able to estimate the mean pulmonary capillary pressure at 7 mmHg. To keep this low-pressure, the vessels walls do not require being as long strong as in the systemic system, but the walls of the pulmonary system are extraordinary thin.

There is not barely difference between the pressure in the left atrium and in the right atrium . However, the pressure drop in the systemic system is so much higher than in the pulmonary system, approximately a factor of 10.

Although the pressure gradient is much lower in the pulmonary circulation system than that of the systemic circulation, both the pulmonary circulation and systemic circulation must drive a blood flow volume as much as the cardiac output, around (5L/min).

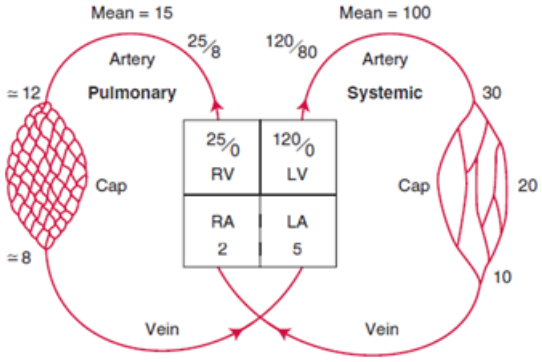

Figure 2.9: Comparison of pressures in the pulmonary and systemic circulation. Adapted from [Wes12]

3 Matlab Simscape

The different models of this thesis were implemented in SIMSCAPE™. SIMSCAPE™ is an object-oriented modeling and simulation module that extends the capability of SIMULINK® providing tools to model and simulate multi-domain physical systems, such as those with electrical, hidraulic, mechanical, thermal and pneumatic componets [MAT]. Simscape language is used under MATLAB® and SIMULINK® environtments. Therefore, it can benefict from MATLAB® functions and SIMULINK® blocks.

The differences between SIMULINK® and SIMSCAPE™ are the followings. SIMULINK® uses an causal modeling approach. This means that their blocks represents mathematical operations or operate on signals. When these blocks are connected together, the resulting diagram represents the mathematical model of the system under consideration. On the other hand, SIMSCAPE™ uses an acausal modeling approach [MAT]. Their blocks represent physical elements, such as resistors and capacitors. Therefore, the model of a system is built in the same way as we would assembled a physical system. In this case, the equations that characterize the behaviour of the real system are created automatically by SIMSCAPE™ from the model.

Fig. 3.1 and Fig.3.2 represent the differences between SIMULINK® and SIMSCAPE™ .

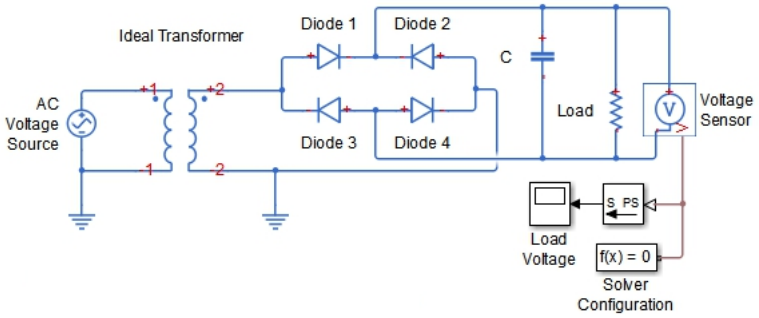

Figure 3.1: A representation of a full-wave bridge rectifier model in Matlab SIMSCAPE™ [MAT]

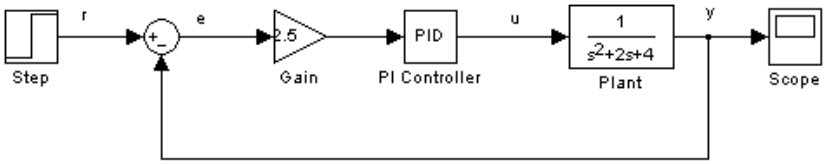

Figure 3.2: A simple model representation using SIMULINK® [MAT]

Fig.3.1 shows an ideal AC transformer plus full-wave bridge rectifier. It converts 120 volts AC to 12 volts DC. The transformer makes the conversion from 120 volts AC to 12 volts AC. Then the full-wave bridge rectifier plus capacitor combination converts the AC signal to DC. On the other hand, Fig.3.2 shows a controller. In this case, the controller is represented by gains and controller transfer functions. Comparing Fig.3.1 and Fig.3.2, we can determinate that SIMSCAPE™ language makes modeling physical system easier and more intuituve than SIMULINK®.

SIMSCAPE™ is accessible as a library within the SIMULINK® environment. This block library contains principally two top-level libraries: Fundation Library and Utilities.

- **Fundation Library** composed of basic blocks in electrical, mechanical, magnetic, thermal, hydraulic and pneumatic engineering.

- **Utilities** composed of environment blocks for creating Physical Network models. For example, converter blocks used to connect SIMSCAPE™ diagrams to SIMULINK® sources and scopes.

The SIMSCAPE™ library can also include more specific domain libreries that belong to the Physical Modeling family: SimElectronic, SimDriveline, SimMechanics, SimHydraulics and SimPowerSystem [MAT]. A representation of the SIMSCAPE™ library is shown in Fig.3.3:

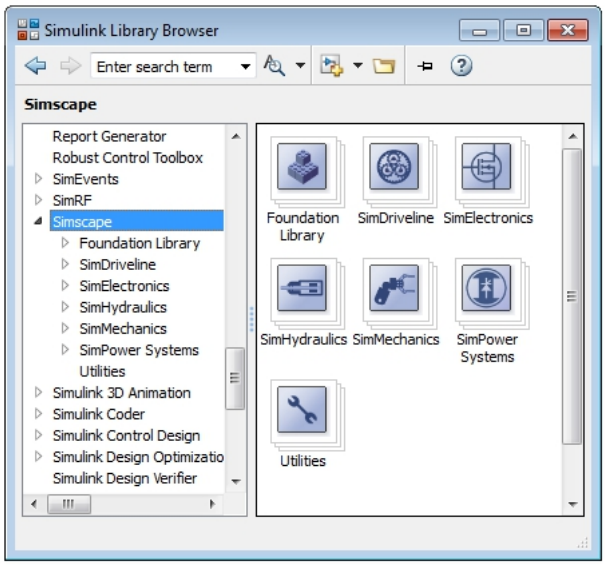

Figure 3.3: SIMSCAPE™ Library [MAT]

We focus in the Electrical Library within the Fundation Library (see Fig.3.4), to explain its distribution. The remaining libraries are similar. Inside of the Electrical group from the library we can differentiate three subgroups: Electrical Elements, Electrical Sources and Electrical Sensors. The Electrical Elements subgroup contains common electrical

components such as Resistor, Indoctor, Capacitor, Mutual Inductor, Ideal Transformer and Variable Resistor are all provided as blocks. The Electrical Sources subgroup contains sources such as AC Source and DC Source while the Electrical Sensors subgroup contains Voltage Sensor and Current Sensor.

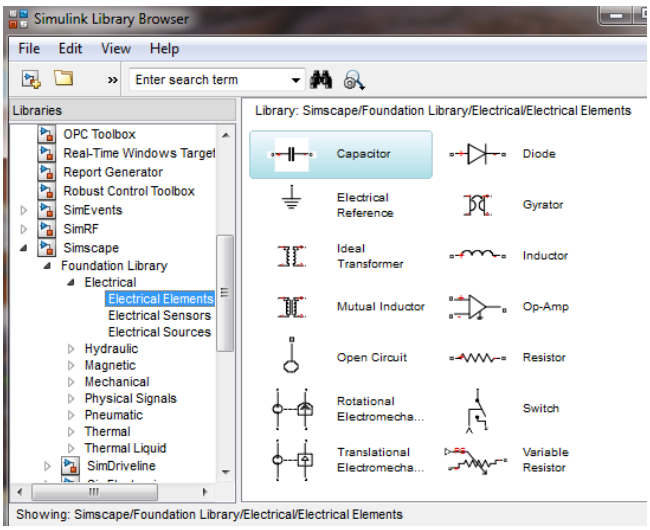

(a) Electrical Elements Subgroup

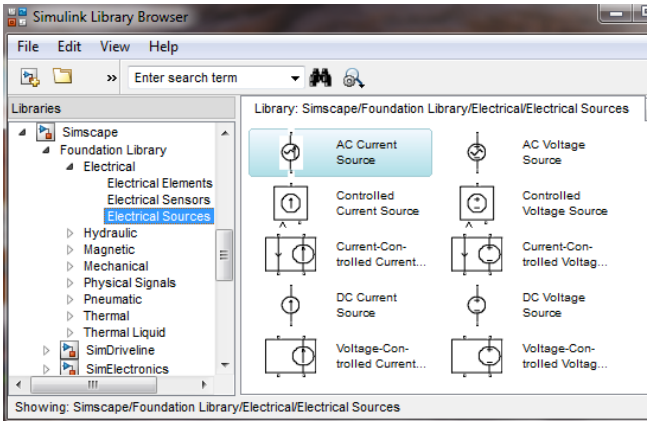

(b) Electrical Sources Subgroup

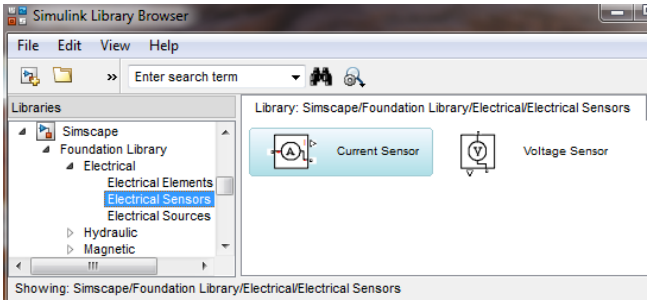

(c) Electrical Sensors Subgroup

Figure 3.4: Electrical Library Simscape

These prebuilt blocks, however, may not be sufficient to the particular purpose and thus, it is necessary extend the existing block libraries. By using the SIMSCAPE™ language, based on the MATLAB® programming language, we can define new customized components or even new physical domains, as textual file. Then the new components are converted into libraries of additional SIMSCAPE™ block that can be used in the model.

A representation of the code of a new component in textual file and the resulting component block and dialog box are shown in Fig.3.5.

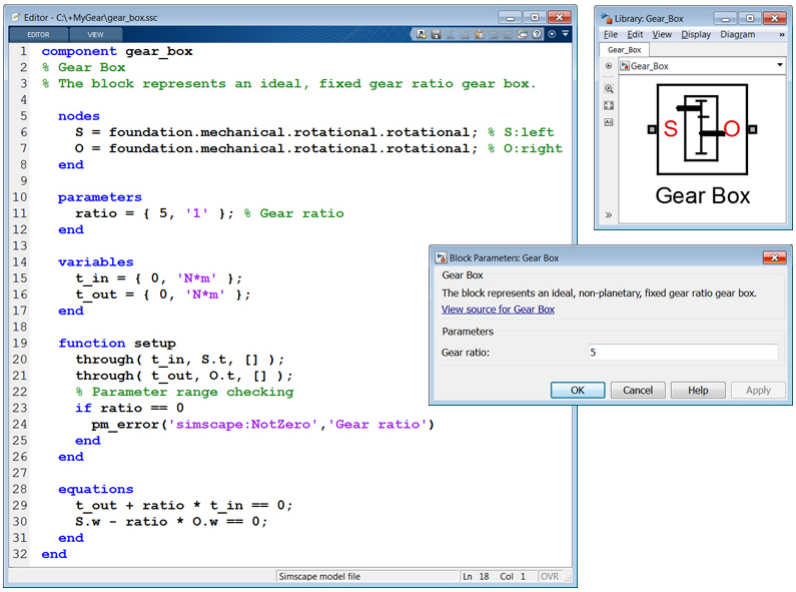

Figure 3.5: A customize component defined by SIMSCAPE™ [MAT]

The code contains a number of modules:

- **Leading statement module**: The block is headed by the keyword **component**. If the novel component is a modification of a component that was in the library, the group that this block belong to is also described in this first sentence.

- **Nodes module**: The nodes of the componet are defined in this module. In this case, two rotational nodes S and O.

- **Dialog parameter setting module**: The **parameters** module is used to define the dialog box for the block. The value and unit of the parameters are described in this module. For instance, in the gear-box block, one parameter is defined, thus the dialog box appears as shown in Fig.3.5. Within the dialog box, one parameter and their units are prompted.

- **Variable declaration module**: The **variable** keyword has to lead a sentence that defines the key variables in the block. In the above code, the variables t_in and t_out are defined.

- **Initial setting module and parameter setting module**: This module is led by **fuction setup**. The value of ratio is examined to see whether it is equal to zero or not. If it is, an error mensage is given. The initial values of t_in and t_out are also assigned in this module.

- **Mathematical model description**: This module is led by the keyword equations and define the behavior of the component.

4 The Perfusion Distribution Model

In this chapter, we develop a new cardiovascular model by focusing on the distribution of the perfusion in the lung. The main goal is to present the gravity effect between different parts of the torax, and how it effects on the perfusion in the lung.

The lung is the unique organ that separates liquid and gas by a thin membrane. The difference of pressure between both substances, which is known as "transmural pressure", varies depending on the vertical level in the lung so that vessels at different levels are subjected to different transmural pressure. This difference of transmural pressure causes that the pulmonary capillary vasculature, characterized by being highly compliant, can exhibit from cessation of flow, when the vessel is collapsed, to different flow rates, as it is shown in Fig.4.2.

This overall behavior, which is known as the "Starling resistor", has been extensively studied by means of a flexible and collapsible tube surrounded by a pressurizable chamber, as it is shown in Fig.4.1. The behavior of the tube can be explained principally due to the influence of three independent pressures: the inlet pressure, P_1 , the outlet pressure, P_2 and the external pressure P_e.

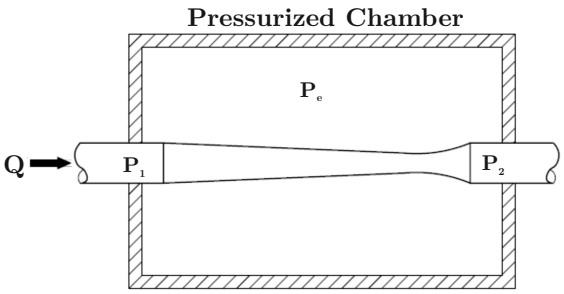

Figure 4.1: The Starling Resistor. P_1: inlet pressure; P_2: outlet pressure; P_e: external pressure; Figure adapted from [Hel04]

We assume an idealized Starling resistor model in which the tube presents the following states:

- initially $P_e > P_1 > P_2$: the tube is collapsed along its entire length, offering infinite resistance to flow. Therefore in this case, the flow is zero:

$$Q(P_e, P_1, P_2) = 0. \tag{4.1}$$

- then $P_1 > P_e > P_2$: the tube inflates at its upstream side, whilst downstream remainds collapsed; in this case, the resistance to the flow falls, R, and the flow is

determined by the difference between the inlet pressure and the external pressure ($P_1 - P_e$), as it is shown in the equation below:

$$Q(P_e, P_1, P_2) = \frac{P_1 - P_e}{R}. \tag{4.2}$$

- finally $P_1 > P_2 > P_e$: the tube is uniformily inflated. The flow in this case is determined by the difference between the inlet and the outlet pressure ($P_1 - P_2$) and the resistance R

$$Q(P_e, P_1, P_2) = \frac{P_1 - P_2}{R}. \tag{4.3}$$

The tube in the mechanical model represented in Fig.4.1, is associated with the pulmonary capillary vasculature in the lung and whose variation of caliber (collapsible or distensible) is due to the gravity. Thus, the inlet and outlet pressures in the Starling resistor model are matched with the pulmonary arterial and venous pressures and the hydrostatic pressure associated to the vertical level in the lung respectively.

All the parameters presented in this section are shown in Tab.4.1

Table 4.1: Parameters used in the lung and pressurized table

Parameter	**Meaning**
P_1	Inlet pressure of pressurized chamber
P_2	Outlet pressure of pressurized chamber
P_e	External pressure of pressurized chamber
P_{inlet}	Inlet pressure in the lung
P_{outlet}	Outlet pressure in the lung
P_{pa}	Pulmonary arterial pressure
P_{pv}	Pulmonary venous pressure
P_{ALV}	Alveolar pressure
P_{Hyd}	Hydrostatic pressure
L	Lung length
ρ	Density of blood
g	Gravity
d	Height of the lung respect the heart level
d_1	Boundary between zone I and II
d_2	Boundary between zone II and III

The inlet pressure in the lung is shown as:

$$P_{\text{inlet}}(t) = P_{\text{pa}}(t) - P_{\text{Hyd}}; \tag{4.4}$$

where hydrostatic pressure (P_{Hyd}) is the product of gravity g, the density of the blood ρ, and the height of the lung respect the heart level d, as it is shown in the following equation:

$$P_{\mathrm{Hyd}} = \rho\, g\, d. \tag{4.5}$$

On the other hand, the outlet pressure is:

$$P_{\mathrm{outlet}}(t) = P_{\mathrm{pv}}(t) - P_{\mathrm{Hyd}}. \tag{4.6}$$

Finally, the external pressure P_{e} is the alveolar pressure:

$$P_{\mathrm{e}}(t) = P_{\mathrm{ALV}}(t). \tag{4.7}$$

The lungs are often divided into zones to describe the effect of gravity on pulmonary capillary blood flow. In our model, the lung are divided into three zones, as the idealized Starling resistor previously decribed and as well as West indicated [Wes12](see Fig.4.2).

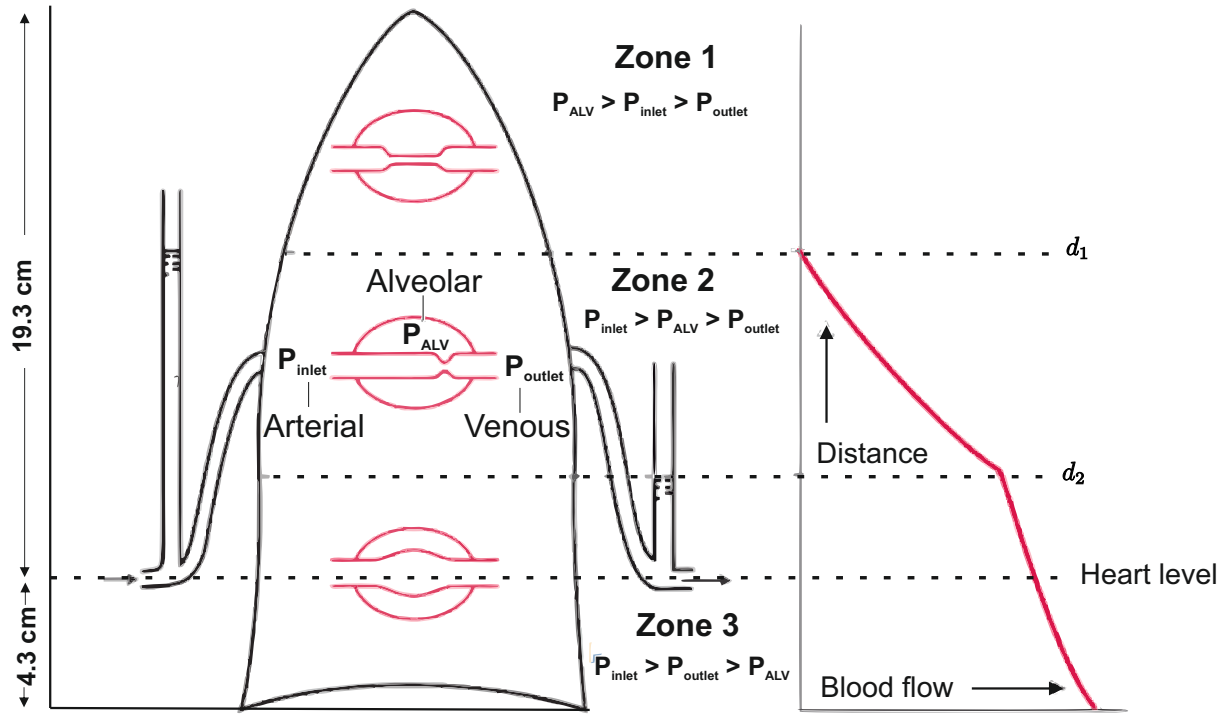

Figure 4.2: Distribution of blood flow in the lung. Figure adapted from [Wes12]

.

As it is shown in Fig.4.2, the first zone (zone 1) is characterized by a complete collapse of the pulmonary capillary vasculature, thus there is no flow in this zone. Further down

the lung, the vessels become open by recruitment (zone 2) and in the third zone (zone 3) the capillaries are already open, but they may be distended according to the transmural pressure. Therefore, the flow increases from the second to the third zone (the base of the uprigth lung). Each zone would be detailed in the following sections.

It is necessary to determinate the vertical lenght of the lung and the location of the zero pressure point in the lung. It has a fundamental role in the calculation of the hydrostatic pressure at different levels in the lung, as well as in the determination of the boundaries between zones. Some authors, such as West [Wes12] and Guyton and Hall [GH12], have estimated the length of the lung around 30 cm. This represents a 23 mmHg pressure difference, where 15mmHg of them are above the level of the mid-left atrium (zero pressure level) and 8 mmHg below. In this thesis we use the average length L = 23.6 cm, estimated by Lewis and Christianson [LC78] in fifteen male patients. From this length, 19.3 cm are located above the level of the main pulmonary artery and vein, while the remaining (20% of the lung) 4.3 cm are situated below the mid-left atrium, as it is shown in Fig.4.2.

Since in the zone I, the alveolar pressure is greater than the inlet pressure, the upper boundary, between zone I and II (d_1), is established when the pulmonary artery pressure (P_{pa}) minus the hydrostatic pressure (Eq. 4.4) is equal to the alveolar pressure, as it is presented in the equation:

$$P_{\mathrm{pa}}(t) - \rho\, g\, d_1(t) = P_{\mathrm{ALV}}(t) \tag{4.8a}$$

$$d_1(t) = \frac{P_{\mathrm{pa}}(t) - P_{\mathrm{ALV}}(t)}{\rho\, g} \tag{4.8b}$$

On the other hand, the boundary between zone II and III (d_2) is established when the pulmonary venous pressure minus the hydrostatic pressure, which is actually the outlet pressure represented in Eq. 4.6, is equal to the alveolar pressure:

$$P_{\mathrm{pv}}(t) - \rho\, g\, d_2(t) = P_{\mathrm{ALV}}(t) \tag{4.9a}$$

$$d_2(t) = \frac{P_{\mathrm{pv}}(t) - P_{\mathrm{ALV}}(t)}{\rho\, g} \tag{4.9b}$$

Both limits have the restriction $d_1(t) \leq \frac{4L}{5} = 19.3$, $d_2(t) \geq \frac{-L}{5} = -4.3$.

4.1 Minimal Model

A minimal model of the pulmonary blood flow distribution is addressed in this section. It is shown in Fig.4.3. This model allows the simulation between pressure and flow where the

hydrostatic pressure is an important factor. Also this model of the pulmonary vasculature is similar to the represetation of a vascular segment of the systemic circulation by Heldt [Hel04].

The pulmonary artery pressure (P_{pa}), which is generated by the right ventricule ejecting blood into the pulmonary circulation, varies during systole and diastole as well as the pulmonary vein pressure. These pressures also suffer variation depending on the vertical level in the lung with respect the left-atrium level. This vertical level produces an increment or decrement in the hydrostatic pressure (P_{Hyd}), and thus affects the pulmonary artery and venous pressures modifying their values, as shown in Fig.4.2. Blood flows through the pulmonary vasculature, which is comprised of three anatomic compartements connected in series: the arterial tree, the capillary bed, and the venular tree. These compartiments are respresented in our model by the resistances R_{a}, R_{c}, R_{v} respectively, and symbolyze the pressure drop throughout the pulmonary vasculature. Also the variation of pressure across the membrane, which separates liquid and gas in the pulmonary capillary vasculature, is represented by a capillary bed compliance C_{cp} that symbolizes the distension and compression of the capillary bed, according to the transmural pressure $\Delta P_{\mathrm{tm}} = P_{\mathrm{cp}} - P_{\mathrm{ALV}}$. Finally, the oxygenated blood returns to the heart by mean of the pulmonary vein whose pressure is the pulmonary vein pressure (P_{pv}). The model is shown in Fig.4.3.

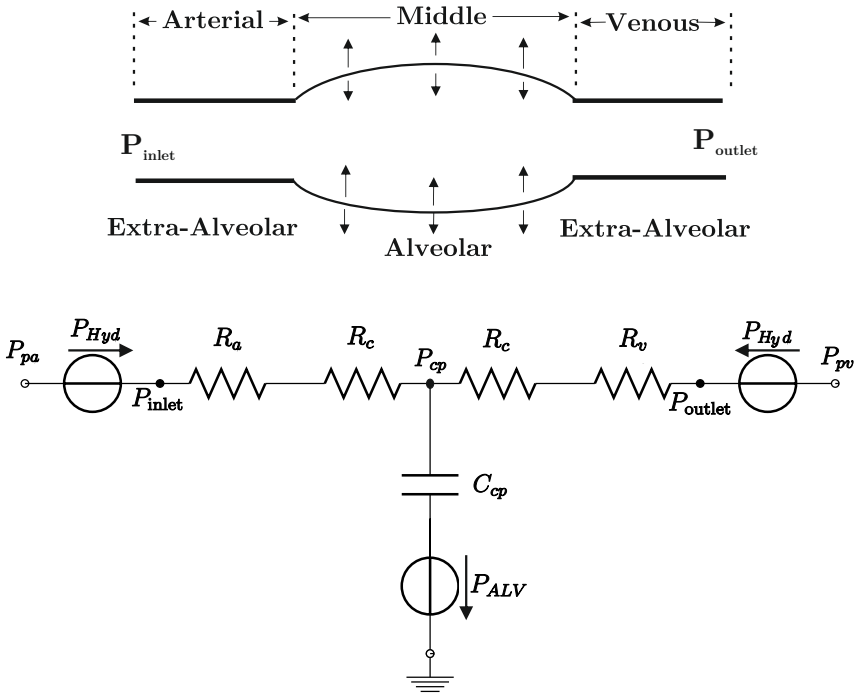

Figure 4.3: A model of pulmonary vasculature relating arterial, capillary and venous segmets

.

This model would be used to represent each single zone of the lung. Since in our thesis the three zones would be developed, upper zone, middle zone and lower zone, the complet model with this zones is shown in Fig.4.4:

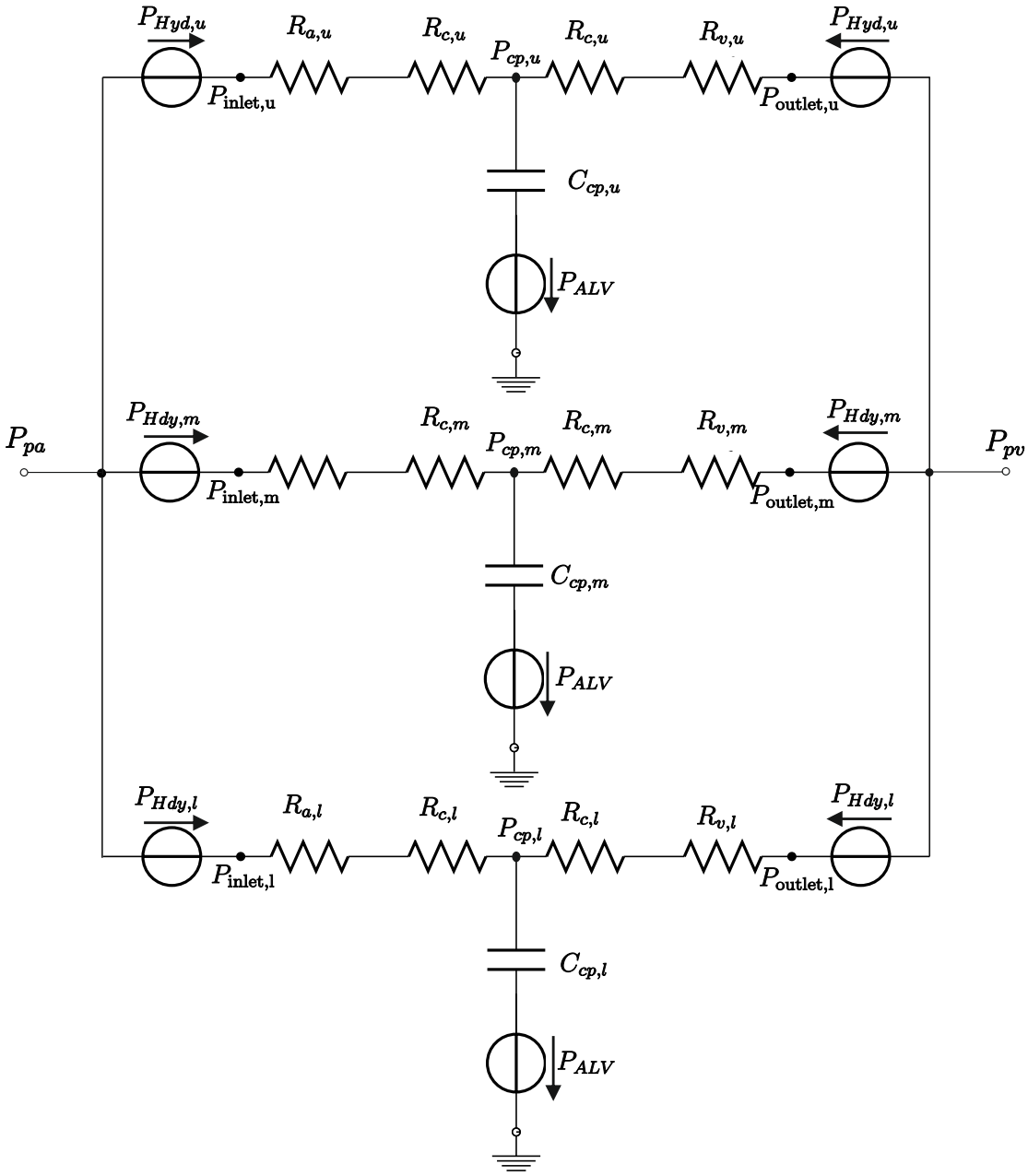

Figure 4.4: Complete model with the three zones of the lung

.

Tab.4.2 shows all the components used in our model of the three zones.

Table 4.2: Parameters of the model

Parameter	Meaning
P_{pa}	Pulmonary arterial pressure
P_{pv}	Pulmonary venous pressure
P_{ALV}	Alveolar pressure
$P_{\mathrm{Hyd,u}}$	Hydrostatic pressure upper zone
$P_{\mathrm{Hyd,m}}$	Hydrostatic pressure middle zone
$P_{\mathrm{Hyd,l}}$	Hydrostatic pressure lower zone
$P_{1,\mathrm{u}}$	Inlet pressure upper zone
$P_{2,\mathrm{u}}$	Outlet pressure upper zone
$P_{1,\mathrm{m}}$	Inlet pressure middle zone
$P_{2,\mathrm{m}}$	Outlet pressure middle zone
$P_{1,\mathrm{u}}$	Inlet pressure lower zone
$P_{2,\mathrm{u}}$	Outlet pressure lower zone
$R_{\mathrm{a,u}}$	Arterial resistance upper zone
$R_{\mathrm{a,m}}$	Arterial resistance middle zone
$R_{\mathrm{a,l}}$	Arterial resistance lower zone
$R_{\mathrm{c,u}}$	Capillary bed resistance upper zone
$R_{\mathrm{c,m}}$	Capillary bed resistance middle zone
$R_{\mathrm{c,l}}$	Capillary bed resistance lower zone
$R_{\mathrm{v,u}}$	Venous resistance upper zone
$R_{\mathrm{v,m}}$	Venous resistance middle zone
$R_{\mathrm{v,l}}$	Venous resistance lower zone
$C_{\mathrm{cp,u}}$	Capillary bed compliance upper zone
$P_{\mathrm{cp,u}}$	Pulmonary capillary pressure upper zone
$C_{\mathrm{cp,m}}$	Capillary bed compliance middle zone
$P_{\mathrm{cp,m}}$	Pulmonary capillary pressure middle zone
$C_{\mathrm{cp,l}}$	Capillary bed compliance lower zone
$P_{\mathrm{cp,l}}$	Pulmonary capillary pressure lower zone
d_{u}	Distance between the heart level and the center of the upper zone
d_{m}	Distance between the heart level and the center of the middle zone
d_{l}	Distance between the heart level and the center of the lower zone
$\bar{d}_1$	Mean of the boundary between zone I and zone II
$\bar{d}_2$	Mean of the boundary between zone II and zone III

In our model, the different vertical levels of the three zones have been established as the midpoint of the respective region, as it is shown in the Fig.4.5. In order to obtain a nominal value of these levels, we consider an static situation where the pulmonary artery pressure, as well as the pulmonary venous pressure and the alveolar pressure are assumed to be the averages. The mean pulmonary artery pressure has a value of 14 mmHg (19.033 cmH_2O)[BP11], the mean pulmonary venous pressure has a value of 1mmHg (1.36 cmH_2O)[BP11] and the value of the mean alveolar pressure is the atmospheric pressure (0 cmH_2O)[GH12]. The following equations represent the different vertical levels, d_u, d_m, d_l respectively. Fig.4.5 also shows the distribution of these distances in the lung.

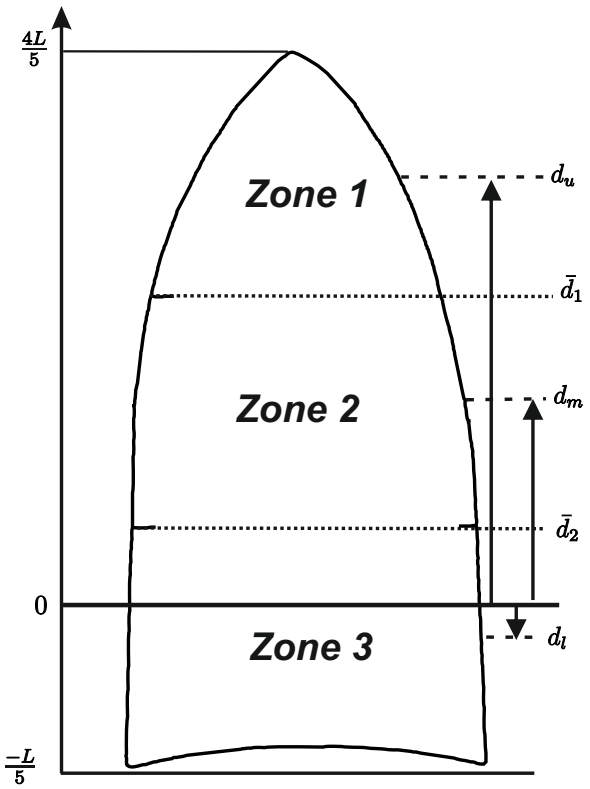

Figure 4.5: Representation of vertical distances between the heart level and the centers of the upper, middle and lower zones

.

$$d_\mathrm{u} = \frac{\frac{4L}{5} - \bar{d}_1}{2} \tag{4.10a}$$

$$d_\mathrm{u} = \frac{\frac{4L}{5} - \frac{\bar{P}_\mathrm{pa} - \bar{P}_\mathrm{ALV}}{\rho\, g\, k}}{2} \tag{4.10b}$$

$$d_\mathrm{m} = \frac{\bar{d}_1 - \bar{d}_2}{2} \tag{4.11a}$$

$$d_{\mathrm{m}} = \frac{\frac{\bar{P}_{\mathrm{pa}} - \bar{P}_{\mathrm{ALV}} - \bar{P}_{\mathrm{pv}} + \bar{P}_{\mathrm{ALV}}}{\rho\, g\, k}}{2} \tag{4.11b}$$

$$d_{\mathrm{l}} = \frac{\bar{d}_2 + \frac{-L}{5}}{2} \tag{4.12a}$$

$$d_{\mathrm{l}} = \frac{\frac{\bar{P}_{\mathrm{pv}} - \bar{P}_{\mathrm{ALV}}}{\rho\, g\, k} + \frac{-L}{5}}{2} \tag{4.12b}$$

d_{l}, d_{m}, d_{l} are described in Tab.4.2 and k is the necessary factor that converts Pa to cmH_2O (1/98.0665).

4.2 Upper Zone

The upper zone is located at the top of the lung and characterized by the fact that the hydrostatic pressure causes that both, the pulmonary arterial and the pulmonary venous pressure, fall below the alveolar pressure ($P_{\mathrm{ALV}} > P_{\mathrm{inlet}} > P_{\mathrm{outlet}}$). Hence, the capillaries are crushed and no flow is driven.

In normal cases, this situation does not occur in healthy people, because the pulmonary artery pressure is sufficient to keep the capillaries partially open and thus, to raise the blood at this part of the lung. This happens during systole, where the value of the pulmonary artery pressure, $P_{\mathrm{pa}} = 25$mmHg, minus the hydrostatic pressure P_{Hdy} difference in the apex (15 mmHg), is greater than the alveolar pressure P_{ALV}:

$$P_{\mathrm{pa}} - P_{\mathrm{Hdy}} \geq P_{\mathrm{ALV}} = 25\,\mathrm{mmHg} - 15\,\mathrm{mmHg} \geq 0\,\mathrm{mmHg} \tag{4.13}$$

Therefore, in these instants of time, the zone 1 has the same behaviour than the zone 2. On the other hand, under condition of reduced pulmonary arterial pressure, such as a severe hemorrhage, or when a patient underlies a mechanical ventilation, where alveolar pressure increases with positive pressure ventilation (PPV), this zone is presented. The zone 1 is also known as alveolar dead space, because it is a ventilated but unperfused area.

The model that represents this region (see Fig.4.6) has to get the flow in this region to be zero. Hence, the resistances of the minimal model $R_{\mathrm{a,u}}$, $R_{\mathrm{c,u}}$, and $R_{\mathrm{v,u}}$, must emulate infinite resistances to offer a high resistance to flow. Moreover, a diode has been introduced with respect the minimal model to avoid the flow goes from the alveolar pressure to the capillary bed.

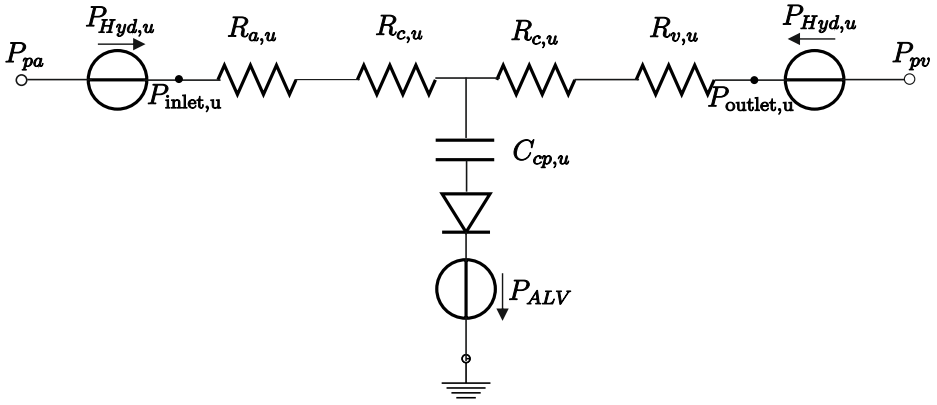

Figure 4.6: Circuit model modified that represent the zone 1

.

4.3 Lower Zone

The zone 3 is characterized by the fact that the flow is purely driven by the difference between the pulmonary artery pressure and the pulmonary vein pressure. In this region, changes in the external pressure (alveolar pressure) have no influence.

Part of the flow was driven through the compliance in the minimal model. As a result the flow is not matched with the difference between inlet and outlet pressures and the alveolar pressure affects the lower zone. In order to avoid it, the model was modified with respect the minimal model (Fig.4.3), as it is shown in Fig.4.7.

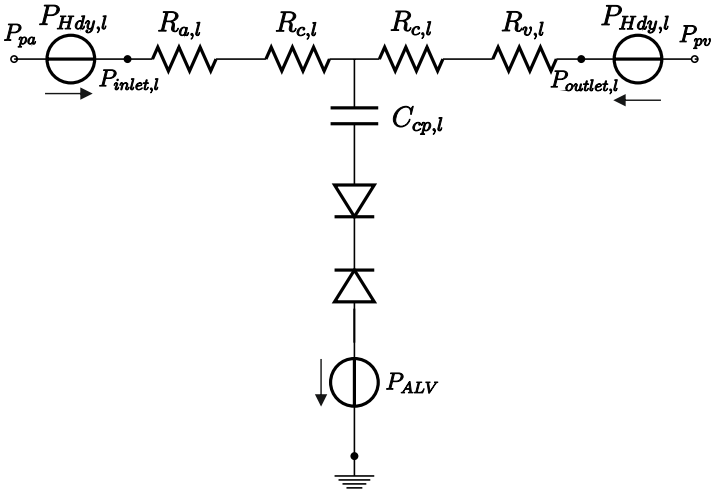

Figure 4.7: Modified model Lower Zone

Two ideal diodes were introduced in the model. With them, the flow remains constant through the circuit as expected and only a small proportion of the total flow goes to the compliance, which represents the distension of the vessel. Thus, the blood flow is

represented by the following equation:

$$q_{\mathrm{l}}(t) = \frac{(P_{\mathrm{pa}}(t) - \rho\, g\, d_{\mathrm{l}}) - (P_{\mathrm{pv}}(t) - \rho\, g\, d_{\mathrm{l}})}{R_{\mathrm{a,l}} + 2R_{\mathrm{c,l}} + R_{\mathrm{v,l}}} \tag{4.14}$$

The longitudinal distribution of pulmonary vasculare resistance (PVR), which consits of the arterial resistance $R_{\mathrm{a,l}}$, the capillary bed resistance $R_{c,l}$, and the venous resistance, $R_{v,l}$, has been studied extensively [BSD68][DGL77]. Nevetheless the results are unalike. It depends on the author and the technique used. The method used by Hakim et al. [HMC82] has been applied in our study to determinate the nominal values of the resistances. They estimated that the middle segment is highly distensible and offers little resistance to the blood flow, 6%-16% of the total PVR, whereas the major fraction of PVR occured in the arterial and venous segments. Using this estimation and the results of Gaar et al. [GTOG67], where 56% of the total PVR was precapillary and 44% postcapillary, the chosen values are: 48% of PVR to the arterial side, $R_{\mathrm{a,l}}$, 16% to the capillaries, $R_{\mathrm{c,l}}$, and 36% to the venous side, $R_{\mathrm{v,l}}$.

Table 4.3: Lower zone Resistances and value

Resistance	Value
$R_{\mathrm{a,l}}$	48 % PVR
$R_{\mathrm{c,l}}$	8 % PVR
$R_{\mathrm{v,l}}$	36 % PVR

Since the blood flow in the zone 1 is zero, the overall blood flow is distributed between the second and the third zone. By using the data proportioned by West et al. [WD60], the flow driving in this zone is approximately $q_{\mathrm{l}} = 3.4\mathrm{L/min}$.

With this flow value and using the average of the pulmonary arterial and venous pressure, the pulmonary vascular resistance can be determined by the following equation:

$$PVR = \sum R_{\mathrm{a,l}} + 2R_{\mathrm{c,l}} + R_{\mathrm{v,l}} = \frac{(\bar{P}_{\mathrm{pa}} - \rho\, g\, d_l) - (\bar{P}_{\mathrm{pv}} - \rho\, g\, d_l)}{q_{\mathrm{l}}} = 310.072\,\mathrm{cmH_2O\,s\,/L} \tag{4.15}$$

4.4 Middle Zone

The zone 2, also known to have a "Waterfall effect", is distinguished by the fact that the pulmonary arterial pressure rises due to the effect of the hydrostatic pressure, and thus, it exceeds the alveolar pressure. However, the pulmonary venous pressure remains lower than the alveolar pressure($P_{\text{inlet}} > P_{\text{ALV}} > P_{\text{outlet}}$).

Due to this condition, the pressure gradient, which determines the blood flow, is described by the difference between the pulmonary artery pressure and the alveolar pressure. As a result, the pulmonary venous pressure has not repercussion on the flow in this region of the lung.

The mechanical model, represented in Fig.4.8, is quite analagous to the flow through a collapsible tube when the pressure surrounding the tube exceeds downstream pressure. A constriction is formed at the distal end, the closure pressure P_{cl} is required to keep the collapsible segment open and is approximately equal to the surrounding pressure ($P_{\text{cl}} = P_{\text{ALV}}$). This is the pressure that limits flow.

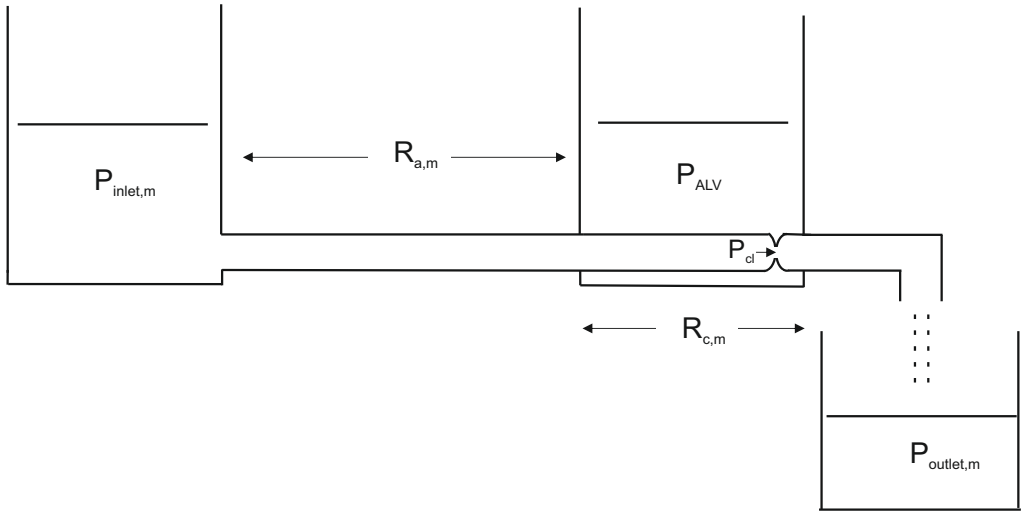

Figure 4.8: Mechanical Model to represent Waterfall effect

.

The minimal model as presented in Sec.4.1 is not adecuated to represent mechanical properties of zone 2. Due to the waterfall effect, the driving flow q_{m} depends only on the pulmonary artery pressure P_{pa}, the hydrostatic pressure P_{Hyd} and the alveolar pressure P_{ALV}. Also, the venous resistance $R_{\text{v,m}}$ does not affect flow, only affects the arterial resistance $R_{\text{a,m}}$ and both capillary resistances $R_{\text{c,m}}$. Because of that, the minimal model in this region was replaced by the following one:

This model is similar to the waterfall model proposed by Downey and Kirk [DK75]. The diode in the electrical analog was introduced to prevent retrogade perfusion, from the

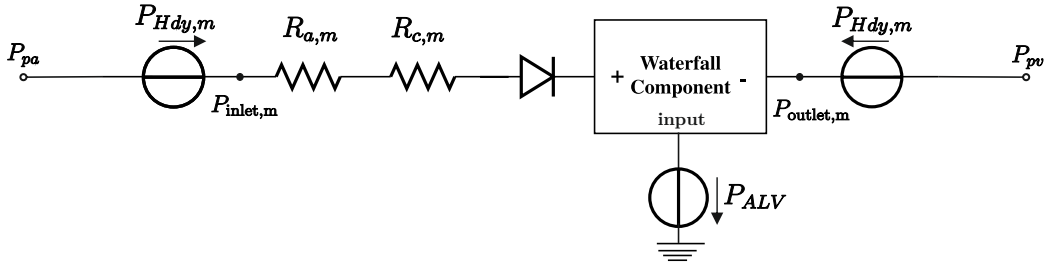

Figure 4.9: Circuit model Waterfall effect

.

venous to the arterial side. The resistances that have influence in this model are $R_{\mathrm{a,m}}$ and $R_{\mathrm{c,m}}$ and, a new component called "Waterfall component" is created in MATLAB SIMSCAPE. This component emulates the alveolar pressure and it allows the flow to be driven to the venous side. The equation that represents the blood flow rate in this section of the lung is:

$$q_{\mathrm{m}}(t) = \frac{P_{\mathrm{pa}}(t) - \rho\, g\, d_m - P_{\mathrm{ALV}}(t)}{R_{\mathrm{a,m}} + R_{\mathrm{c,m}}} \tag{4.16}$$

As well as in the previous section, the data proportioned by West et al. [WD60] has been used to determine the flow in the second zone, it is approximately $q_{\mathrm{m}} = 1.9\mathrm{L/min}$. Also, the average of the pulmonary arterial pressure and alveolar pressure, have been applied to calculate the values of $R_{\mathrm{a,m}}$ and $R_{\mathrm{c,m}}$:

$$PVR = \sum R_{\mathrm{a,m}} + R_{\mathrm{c,m}} = \frac{(\bar{P}_{\mathrm{pa}} - \rho\, g\, d_l) - \bar{P}_{\mathrm{ALV}}}{q_{\mathrm{m}}} = 279.06\,\mathrm{cmH_2O\,s\,/L} \tag{4.17}$$

Since the venous resistance has no influence in this lung region, its proportional value is equally divided between the arterial and capillary resistance. Therefore, the value of $R_{\mathrm{a,m}}$ is 66% of PVR while the value of $R_{\mathrm{c,m}}$ is 38%.

Table 4.4: Middle Zone Resistances and value

Resistance	Value
$R_{\mathrm{a,m}}$	66 % PVR
$R_{\mathrm{c,m}}$	38 % PVR

The resultant circuit that represents the three zones is shown in Fig.4.10:

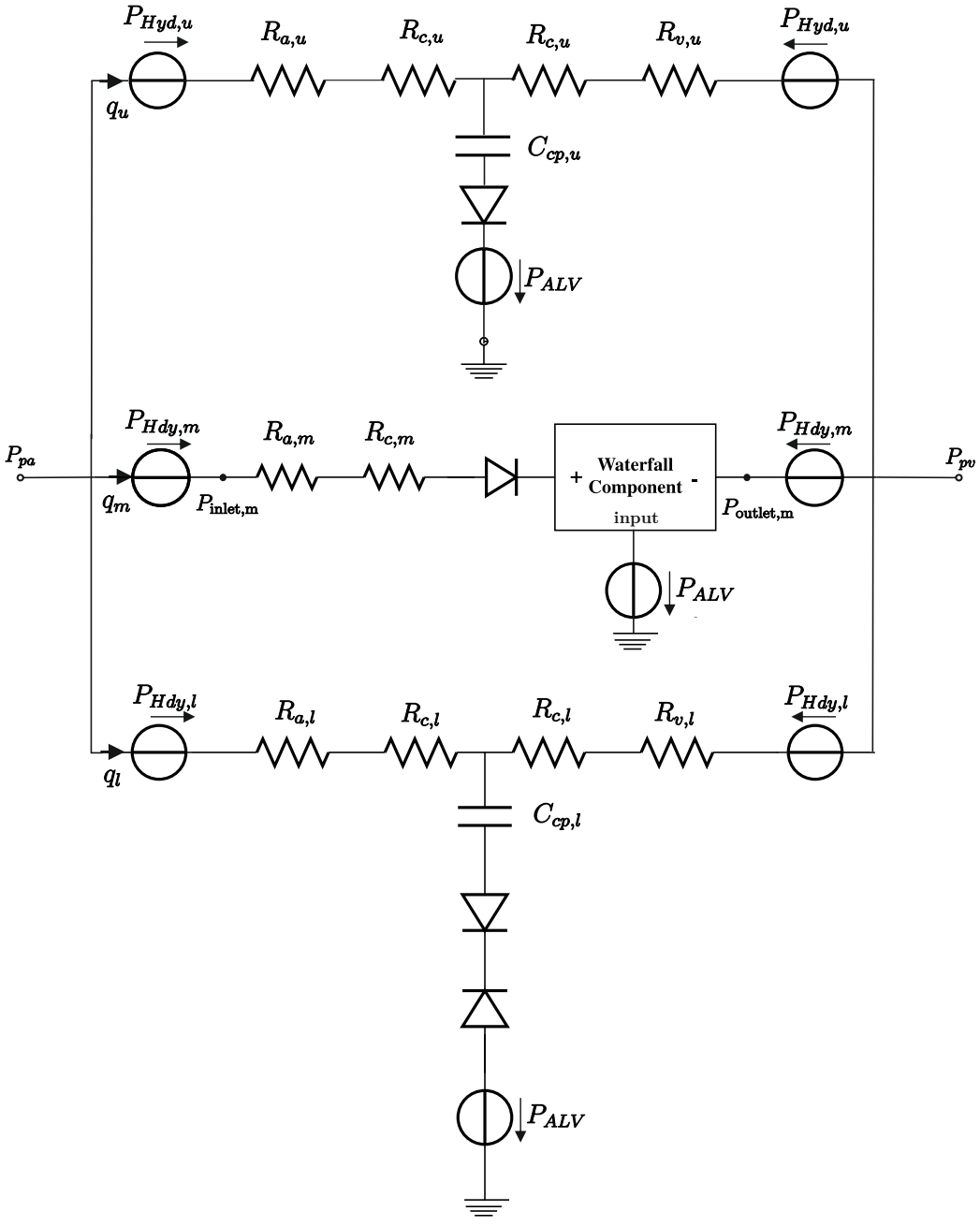

Figure 4.10: Circuit model modified that represent the three Zones

.

5 The Ventilation Distribution Model

In this chapter a model of ventilation distribution in the human lung is developed. Although Otis et al. [OMB+56] were the first to made a theoretical approximation of the distribution and ventilation within the lungs, the model developed in these study is based upon the two-lobe ventilation theory of Pedley et al. [PSME72], where some vertical variation in the distribution of ventilation were considered. In our case, the upright human lung is divided into three different vertical lobes, according to the three vertical zones of the blood flow distribution described in the previous chapter. These lobes correspond to **Upper lobe**, **Middle lobe** and **Lower lobe** respectively, as they are shown in Fig.5.1.

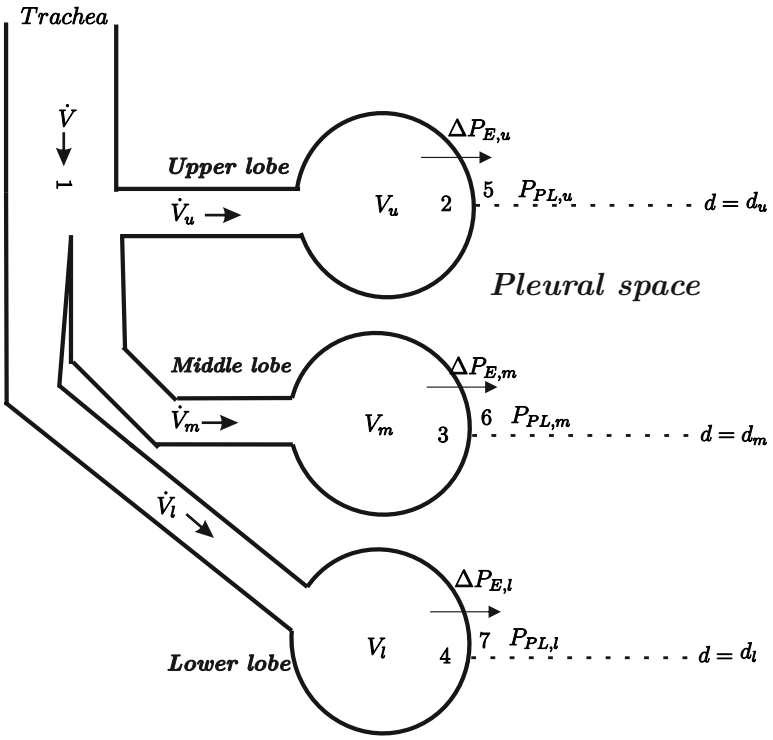

Figure 5.1: Three compartiment model of the lung developed in this chapter

The physiological behavior model of the ventilation in the lung is described in Fig.5.1. When we inhale, the airflow is driven from the mouth or nose to the trachea and distributed between the three compartiments simultaneously. Because of the inspiration, the volumen of the lung increase, which causes changes in the pleural pressure as well as in the elastic properties of the lung.

Therefore, we can determinate that each compartiment is characterized by their flow-resistive and volume-elastic properties as well as the corresponding pleural pressure, which depends on the vertical distance. The resultant electrical circuit analogue to this physiological behavior is represented in Fig.5.2:

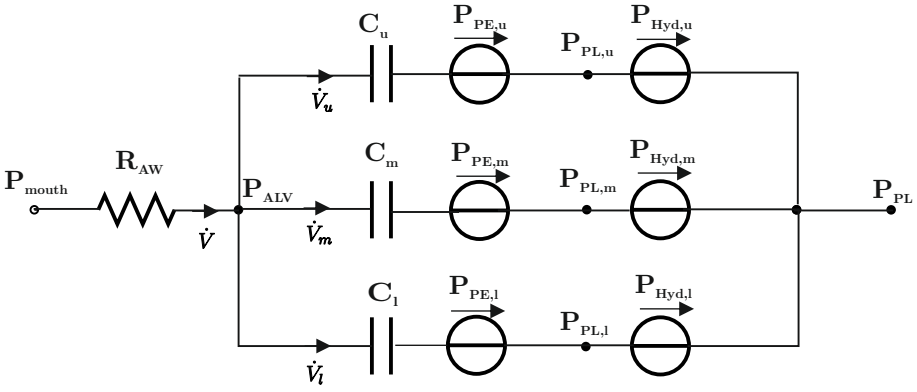

Figure 5.2: Electrical circuit equivalent to the ventilation distribution model developed

.

We have assumed that the alveolar pressure would change equally in all the compartiments. Therefore, the resistive properties of the lung, which represent the pressure drop from the bifurcation (point 1) to the alveoli (point 2, 3 or 4) in Fig.5.1, would be the same. These three resistances in parallel are represented in the circuit as a unique resistance, R_{AW}. On the other hand, the compliances C_{u}, C_{m} and C_l represent the elastic pressure drops across lung walls for the upper, middle and lower lobes respectively (between points 2 and 5, points 3 and 6 and points 4 and 7 in Fig.5.1). The sources $P_{\mathrm{Hdy,u}}$, $P_{\mathrm{Hdy,m}}$, $P_{\mathrm{Hdy,l}}$ and the pleural pressure in the center of the lung simbolize the different pleural pressures for each lobe due to the vertical variations. Finally, the pleural extended pressure sources $P_{\mathrm{PE,u}}$, $P_{\mathrm{PE,m}}$, $P_{\mathrm{PE,l}}$ represent the prestress of the elastic lung and chest wall in the upper zone, middle zone and lower zone respectively. These are calculated as:

$$P_{\mathrm{PE,u}} = -2P_{\mathrm{PL,u}} \tag{5.1a}$$

$$P_{\mathrm{PE,m}} = -2P_{\mathrm{PL,m}} \tag{5.1b}$$

$$P_{\mathrm{PE,l}} = -2P_{\mathrm{PL,l}} \tag{5.1c}$$

Extending the equation developed by Pedley et al [PSME72] for the pressure balance between the two lobes to the three lobes, and neglecting the resistive pressures drop because are the same in the three pathways, the following equation is derived:

$$\Delta P_{\mathrm{E,u}}(t) + P_{\mathrm{PL,u}}(t) = \Delta P_{\mathrm{E,m}}(t) + P_{\mathrm{PL,m}}(t) = \Delta P_{\mathrm{E,l}}(t) + P_{\mathrm{PL,l}}(t), \tag{5.2}$$

where $\Delta P_{\mathrm{E,u}}$, $\Delta P_{\mathrm{E,m}}$, $\Delta P_{\mathrm{E,l}}$ are the elastic pressured drops and $P_{\mathrm{PL,u}}$, $P_{\mathrm{PL,m}}$, $P_{\mathrm{PL,l}}$ are the pleural pressures at different levels of the lung.

Moreover the sum of the three flows $\dot{V}_{\mathrm{u}}$, $\dot{V}_{\mathrm{m}}$, $\dot{V}_{\mathrm{l}}$ must be equal to the overall flow rate, as is shown in the equation:

$$\dot{V}_{\mathrm{u}}(t) + \dot{V}_{\mathrm{m}}(t) + \dot{V}_{\mathrm{l}}(t) = \dot{V}(t) \tag{5.3}$$

In addition the sum of the volumes in each lobe V_{u} , V_{m} and V_{l} must be equal to the whole lung volume V:

$$V_{\mathrm{u}}(t) + V_{\mathrm{m}}(t) + V_{\mathrm{l}}(t) = V = V_0 + \dot{V}_t(t) \tag{5.4}$$

Where t represents the time elapsed since the inspiration begins and V_0 is the initial total volume, usually taken to be the volume in resting position (FRC). Functional residual capacity is the volumen at the end of a normal exhalation. Besides the elastic recoil forces of the lung and chest wall are in equilibrium.

All the components and parameters described in this section is shown in Tab.5.1:

Table 5.1: Parameters

Parameter	Meaning
P_{mouth}	Mouth pressure equals to atmospheric pressure
R_{AW}	Overall airway resistance
P_{ALV}	Alveolar pressure
C_{u}	Upper lobe compliance
C_{m}	Middle lobe compliance
C_{l}	Lower lobe compliance
$P_{\text{PL,u}}$	Upper lobe pleural pressure
$P_{\text{PL,m}}$	Middle lobe pleural pressure
$P_{\text{PL,l}}$	Lower lobe pleural pressure
$P_{\text{PE,u}}$	Upper lobe pleural extended pressure
$P_{\text{PE,m}}$	Middle lobe pleural extended pressure
$P_{\text{PE,l}}$	Lower lobe pleural extended pressure
$P_{\text{Hyd,u}}$	Hydrostatic pressure upper zone
$P_{\text{Hyd,m}}$	Hydrostatic pressure middle zone
$P_{\text{Hyd,l}}$	Hydrostatic pressure lower zone
P_{PL}	Pleural pressure
$\Delta P_{\text{E,u}}$	Upper lobe elastic pressure drop or transmural pressure
$\Delta P_{\text{E,m}}$	Middle lobe elastic pressure drop or transmural pressure
$\Delta P_{\text{E,l}}$	Lower lobe elastic pressure drop or transmural pressure
$\dot{V}_{\text{u}}$	Upper lobe Airflow
$\dot{V}_{\text{m}}$	Middle lobe Airflow
$\dot{V}_{\text{l}}$	Lower lobe Airflow
V	Lung volume
V_{u}	Upper lobe Volume
V_{m}	Middle lobe Volume
V_{l}	Lower lobe Volume
V_0	Initial total volume (V_{FRC})
d_{u}	Distance between the center of the lung and the center of the upper lobe
d_{m}	Distance between the center of the lung and the center of the middle zone
d_{l}	Distance between the center of the lung and the center of the lower zone

5.1 Determination of compliances

The pressure-volume curve is non-lineal according to Mead [Mea61], Salazar and Knowles [SK64], and Milic-Emili et al. [MEHD+66]. The Fig. 5.3 represents the mean pressure-volume curve obtained by Salazar et al. [SK64] in the analisys of 20 normal subjects.

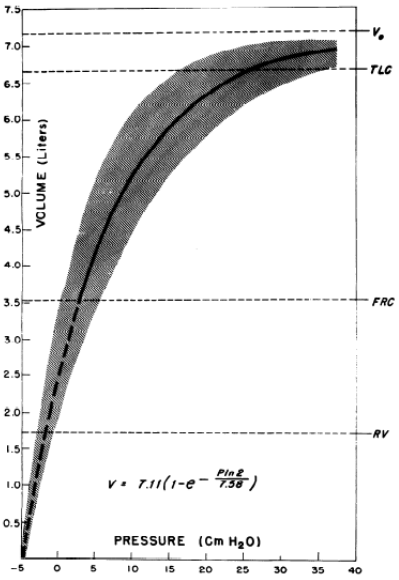

Figure 5.3: Mean PV curve for the group of 20 normal subjects [SK64]

.

The exponential form used to represent this curvilinear relation of pressure and volume changes is shown:

$$V(t) = V_o(1 - e^{-k\,\Delta P_{\mathrm{E}}(t)}), \tag{5.5}$$

where V is the total volume, ΔP_{E} is the transpulmonary pressure of the lung , V_o represents the maximal pulmonary volume, the volume at which the slope is zero, and k is the elastic costant which define the slope of the P-V curve. This formula is used to express the elastic pressure drops for the upper lobe, middle lobe and lower lobe. Isolating the transpulmonary pressure to get the equation in funtion of the volume:

$$\Delta P_{\mathrm{E}}(t) = -\frac{1}{k}\ln\left(1 - \frac{V(t)}{V_o}\right) \tag{5.6}$$

The maximal pulmonary volume V_o at infinite transpulmonary pressure is also defined as a percented (m) of total lung capacity (TLC), as Milic-Emili et al. [MEHD+66] and Pedley et al. [PSME72] indicated. The resulting equation is:

$$\Delta P_{\mathrm{E}}(t) = -\frac{1}{k} \ln \left(1 - \frac{V(t)}{m\,\mathrm{TLC}}\right) \tag{5.7}$$

k and m are the same in the three lobes because the intrinsic elastic properties are assumed to be the same for each lobe [SKME68].

Therefore, the elastic pressure drop for the upper lobe, middle lobe and lower lobe are derived as:

$$\Delta P_{\mathrm{E,u}}(t) = -\frac{1}{k} \ln \left(1 - \frac{V_u(t)}{m\,\mathrm{TLC_u}}\right) \tag{5.8}$$

$$\Delta P_{\mathrm{E,m}}(t) = -\frac{1}{k} \ln \left(1 - \frac{V_m(t)}{m\,\mathrm{TLC_m}}\right) \tag{5.9}$$

$$\Delta P_{\mathrm{E,l}}(t) = -\frac{1}{k} \ln \left(1 - \frac{V_l(t)}{m\,\mathrm{TLC_l}}\right) \tag{5.10}$$

Where V_u, V_m, V_l and $\mathrm{TLC_u}$, $\mathrm{TLC_m}$, $\mathrm{TLC_l}$ are the regional lung volumes and the regional total lung capacities of the upper lobe, middle lobe and lower lobe respectively.

The compliance have been introduced to express the relation between the volume and pressure changes and it is taken as the slope of the Pressure-Volume curve ($\Delta V/\Delta P$), as it is shown in Fig.5.4. The compliance of each lobe is calculated as the slope of the lobar P-V curve at the centre of the lobe.

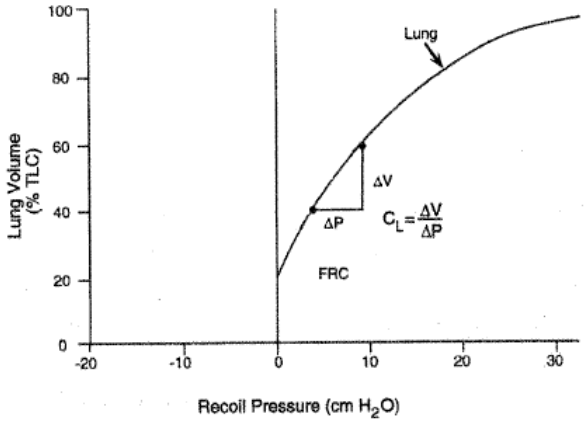

Figure 5.4: Compliance of the lung

.

First of all, the equation of the volume in the upper lobe is defined as:

$$V_{\mathrm{u}}(t) = m\,\mathrm{TLC}_{\mathrm{u}}\,(1 - e^{-k\,\Delta P_{\mathrm{E,u}}(t)}). \tag{5.11}$$

Thus, the compliance in the upper lobe is:

$$C_u = \frac{dV_u}{d(\Delta P_{\mathrm{E,u}})} = k\,m\,\mathrm{TLC}_{\mathrm{u}} e^{-k\,\Delta P_{\mathrm{E,u}}} \tag{5.12}$$

It should be pointed out that Milic-Emili et al. [MEHD$^+$66] established the difference between the transpulmonary pressure at any level along the lung according to the following expression:

$$\Delta P_{\mathrm{E}}(t) - \Delta P_{\mathrm{i}}(t) = -\frac{1}{k}\ln(1 - b\,\Delta D) \tag{5.13}$$

Where ΔP_{E} is the value of the transpulmonary pressure whose height is ΔD (cm) above the isovolume point. ΔP_i is the transulmonary pressure in the isovolume point (the center of the whole lung) and b is a constant which it represent the rate of change of the regional fractional lung volume with the vertical distance, whose average value is 0.023 cm^{-1}[MEHD$^+$66][BMEP66]. In Fig.5.5, a representation of the isovolume point and the different distances d_{u}, d_{m}, d_{l} respect this point are presented.

Therefore, redefining the compliance in the upper lobe in terms of d_{u} and combining the Eq.5.12 and Eq. 5.13 where $\Delta D = \mathrm{d_u}$:

$$C_u = k\,m\,\mathrm{TLC}_{\mathrm{u}}(1 - b\,d_u)e^{-k\,\Delta P_{\mathrm{i}}} \tag{5.14}$$

Similar equations for C_m and C_l:

$$C_m = k\,m\,\mathrm{TLC}_{\mathrm{m}}(1 - b\,d_m)e^{-k\,\Delta P_{\mathrm{i}}} \tag{5.15}$$

$$C_l = k\,m\,\mathrm{TLC}_{\mathrm{l}}(1 - b\,d_l)e^{-k\,\Delta P_{\mathrm{i}}} \tag{5.16}$$

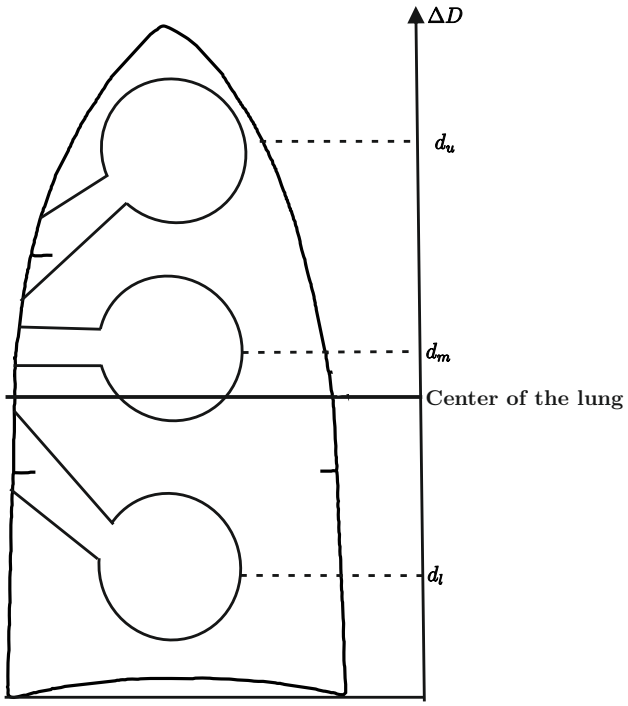

Figure 5.5: Representation of the upper, middle and lower distances respect the center of the lung

.

The pressure-volume curve showed in Fig.5.3 has a linear behaviour between the point situated when the lung is at resting position (FRC) and the point that represents the tidal volume (V_T), the volume of air inhaled and exhaled during normal breath. Since we would assume a normal inspiration and expiration in this thesis, the slope in this part of the pressure-curve is constant and thus, the defined compliances.

The choice of TLC_u, TLC_m TLC_l, d_u, d_m, d_l, k, m, ΔP_i and the values of the compliances are detailed in the Sec.5.5.

5.2 Determination of the hydrostatic pressures

In this section, the pleural and hydrostatic pressures in the upper lobe, middle lobe and lower lobe are determinated. The following equation expresses the transpulmonary pressure in terms of the pleural and alveolar pressures:

$$\Delta P_E(t) = P_{ALV}(t) - P_{PL}(t). \tag{5.17}$$

Thus, the transpulmonary pressure in each lobe is determined by the respectives pleural

pressures:

$$\Delta P_{\mathrm{E_{u,m,l}}}(t) = P_{\mathrm{ALV}}(t) - P_{\mathrm{PL_{u,m,l}}}(t) \tag{5.18}$$

Moreover, the transpulmonary pressure at any level along the lung was also expressed in Eq. 5.13. Combining Eq.5.13 and Eq.5.18, the transpulmonary pressure in the upper lobe is described as:

$$\Delta P_{\mathrm{E_u}}(t) = P_{\mathrm{ALV}}(t) - P_{\mathrm{PL_u}}(t) = -\frac{1}{k}\ln(1 - b\,d_u) + \Delta P_{\mathrm{i}}(t) \tag{5.19}$$

where ΔP_{i} represents the transpulmonary pressure in the center of the lung and it could be also expressed in terms of the pleural and alveolar pressures. Isolating the pleural pressure in the upper lobe:

$$P_{\mathrm{ALV}}(t) - P_{\mathrm{PL_u}}(t) = -\frac{1}{k}\ln(1 - b\,d_u) + (P_{\mathrm{ALV}}(t) + P_{\mathrm{PL}}(t)) \tag{5.20a}$$

$$P_{\mathrm{PL_u}}(t) = \frac{1}{k}\ln(1 - b\,d_u) + P_{\mathrm{PL}}(t) \tag{5.20b}$$

We determine the hydrotatic pressure as the difference between the pleural pressure at any point of the lung and the pleural pressure in the center of the lung. Therefore, the hydrostatic pressures for the three lobes are:

$$P_{\mathrm{Hyd_u}} = \frac{1}{k}\ln(1 - b\,d_u) \tag{5.21}$$

$$P_{\mathrm{Hyd_m}} = \frac{1}{k}\ln(1 - b\,d_m) \tag{5.22}$$

$$P_{\mathrm{Hyd_l}} = \frac{1}{k}\ln(1 - b\,d_l) \tag{5.23}$$

Where d_u, d_m and d_l are the vertical distances [cm] from the isovolume point (see Fig.5.5). Hence, the pleural pressure in each zone is determined by the sum of the hydrostatic and pleural pressure.

5.3 Regional Rate of Alveolar Ventilation

The alveolar ventilation needs to be calculated in order to analyze the ventilation-perfusion ratio in the whole lung, likewise each lobe. Thus, this section is dedicated to determinate the overall lung alveolar ventilation as well as the regional alveolar ventilation.

First of all, the expression of alveolar ventilation per breath is shown in the following equation:

$$\mathrm{V_A} = \mathrm{V_T} - \mathrm{V_D} \tag{5.24}$$

Where $\mathrm{V_D}$ means the dead space volume, whose value is approximately 0.150 Liters [GH12]. On the other hand, $\mathrm{V_T}$ represents the tidal volume, the volume of air inhaled or exhaled during a breath,with a value approximately of 0.5 Liters [GH12]. It can be calculated from de overall airflow using the following equations. A graph example of airflow by [Bat09] is also shown in Fig.5.6.

$$\dot{V}(t) = \frac{P_{\mathrm{mouth}}(t) - P_{\mathrm{ALV}}(t)}{R_{\mathrm{AW}}} \tag{5.25}$$

P_{mouth} is the airway opening pressure, with a value of 0 $\mathrm{cmH_2O}$ (relative to atmospheric pressure), P_{ALV} corresponds to the alveolar pressure and R_{AW} is the resistance of the airways.

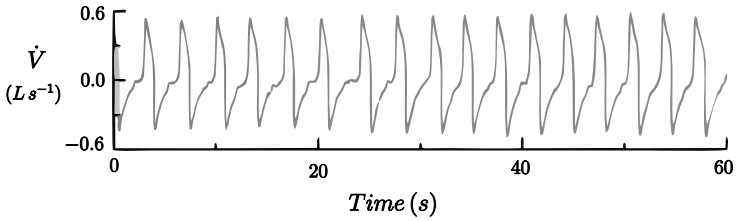

Figure 5.6: Flow measured from a mechanically ventilated patient by [Bat09]

.

The resulting volume is obtained integrating the airflow:

$$V(t) = \int \dot{V}(t)dt \tag{5.26}$$

V represent the variation of volume from FRC during the breath (represented in Fig.5.7 as 0.0 Liters). The volume according to the airflow of the Fig.5.6 is shown in Fig.5.7:

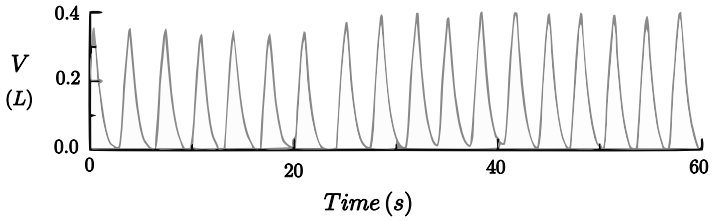

Figure 5.7: Volume measured from a mechanically ventilated patient by [Bat09]

.

Once the tidal volume have been determined (the difference of volumen between the volumen at resting position and the volumen after the inspiration), the alveolar ventilation is obtained by the next equation:

$$\dot{V}_{\mathrm{A}}(t) = V_{\mathrm{A}}(t) * f_{\mathrm{resp}} \tag{5.27}$$

The f_{resp} represents the breath rate per second. Guyton et al.[GH12] established a normal value of (12 [breath min^{-1}]) but in our thesis we have chosen value is 0.3 [breath s^{-1}] (18 [breath min^{-1}]). Alveolar ventilation ($\dot{V}_{\mathrm{A}}$) is measured in [$\mathrm{L\,s}^{-1}$].

In order to calculate the regional alveolar ventilation, the regional alveolar ventilation per breath are needed. They are derivaded from the succesive equations:

$$V_{\mathrm{A,u}}(t) = V_A(t) \; * \; \frac{max\left(\int \dot{V}_u(t)\,dt\right)}{max\left(\int \dot{V}(t)\,dt\right)} \tag{5.28}$$

$$V_{\mathrm{A,m}}(t) = V_A(t) \; * \; \frac{max\left(\int \dot{V}_m(t)\,dt\right)}{max\left(\int \dot{V}(t)\,dt\right)} \tag{5.29}$$

$$V_{\mathrm{A,L}}(t) = V_A(t) \; * \; \frac{max\left(\int \dot{V}_l(t)\,dt\right)}{max\left(\int \dot{V}(t)\,dt\right)} \tag{5.30}$$

Finally, the alveolar ventilation in each lobe is calculated multiplying the respective alveolar volumen and the breath rate.

$$\dot{V}_{\mathrm{A,u}}(t) = V_{\mathrm{A,u}}(t) * f_{\mathrm{resp}} \tag{5.31}$$

$$\dot{V}_{\mathrm{A,m}}(t) = V_{\mathrm{A,m}}(t) * f_{\mathrm{resp}} \tag{5.32}$$

$$\dot{V}_{\mathrm{A,l}}(t) = V_{\mathrm{A,l}}(t) * f_{\mathrm{resp}} \tag{5.33}$$

5.4 Parameterization

In this section we determinate the initial conditions of the regional volumen. When the time $t = 0$, the overall lung volume is equal to the initial total volume ($V = V_0$), also the lung is in equilibrium with no air flowing, thus:

$$\dot{V}_u(t=0) = \dot{V}_m(t=0) = \dot{V}_l(t=0) = \dot{V}(t=0) = 0 \tag{5.34}$$

Combining this equations with Eq.5.2, the three lobar volumes at this conditions $V_u(t=0)$,$V_m(t=0)$, $V_l(t=0)$ are determined.

The procedure to obtain $V_u(t=0)$ are detailed in the following equations. Considering $\Delta P_{\mathrm{E,u}} + P_{\mathrm{PL,u}} = \Delta P_{\mathrm{E,m}} + P_{\mathrm{PL,m}}$ and also, $\Delta P_{\mathrm{E,u}} + P_{\mathrm{PL,u}} = \Delta P_{\mathrm{E,l}} + P_{\mathrm{PL,l}}$:

$$-\frac{1}{k}\ln\left(1-\frac{V_u(t=0)}{m\mathrm{TLC_u}}\right) + P_{\mathrm{PL,u}} = -\frac{1}{k}\ln\left(1-\frac{V_m(t=0)}{m\mathrm{TLC_m}}\right) + P_{\mathrm{PL,m}} \tag{5.35}$$

$$-\frac{1}{k}\ln\left(1-\frac{V_u(t=0)}{m\mathrm{TLC_u}}\right) + P_{\mathrm{PL,u}} = -\frac{1}{k}\ln\left(1-\frac{V_l(t=0)}{m\mathrm{TLC_l}}\right) + P_{\mathrm{PL,l}} \tag{5.36}$$

Isolating each equation separately:

$$\ln\frac{\left(1-\frac{V_m(t=0)}{m\mathrm{TLC_m}}\right)}{\left(1-\frac{V_u(t=0)}{m\mathrm{TLC_u}}\right)} = k(P_{\mathrm{PL,m}} - P_{\mathrm{PL,u}}) \tag{5.37}$$

$$\ln\frac{\left(1-\frac{V_l(t=0)}{m\mathrm{TLC_l}}\right)}{\left(1-\frac{V_u(t=0)}{m\mathrm{TLC_u}}\right)} = k(P_{\mathrm{PL,l}} - P_{\mathrm{PL,u}}) \tag{5.38}$$

And thus,

$$1-\frac{V_m(t=0)}{m\mathrm{TLC_m}} = e^{k(P_{\mathrm{PL,m}}-P_{\mathrm{PL,u}})}\left(1-\frac{V_u(t=0)}{m\mathrm{TLC_u}}\right) \tag{5.39}$$

$$1 - \frac{V_l(t=0)}{m\mathrm{TLC_l}} = e^{k(P_{\mathrm{PL,l}} - P_{\mathrm{PL,u}})} \left(1 - \frac{V_u(t=0)}{m\mathrm{TLC_u}}\right) \tag{5.40}$$

Isolating V_m and V_l in terms of V_u:

$$V_m(t=0) = \left(1 - e^{k(P_{\mathrm{PL,m}} - P_{\mathrm{PL,u}})} \left(1 - \frac{V_u(t=0)}{m\mathrm{TLC_u}}\right)\right) m\mathrm{TLC_m} \tag{5.41}$$

$$V_l(t=0) = \left(1 - e^{k(P_{\mathrm{PL,l}} - P_{\mathrm{PL,u}})} \left(1 - \frac{V_u(t=0)}{m\mathrm{TLC_u}}\right)\right) m\mathrm{TLC_l} \tag{5.42}$$

And also considering that,

$$V_u(t=0) + V_m(t=0) + V_l(t=0) = V_0 \tag{5.43}$$

Combining Eq.5.41 and Eq.5.43:

$$V_0 - V_u(t=0) - V_l(t=0) = \left(1 - e^{k(P_{\mathrm{PL,m}} - P_{\mathrm{PL,u}})} \left(1 - \frac{V_u(t=0)}{m\mathrm{TLC_u}}\right)\right) m\mathrm{TLC_m} \tag{5.44}$$

Remplazing the value V_l of the Eq.5.42 into Eq.5.44:

$$\begin{aligned} V_0 + m\mathrm{TLC_m}\left(e^{k(P_{\mathrm{PL,m}} - P_{\mathrm{PL,u}})} - 1)\right) + m\mathrm{TLC_l}\left(e^{k(P_{\mathrm{PL,l}} - P_{\mathrm{PL,u}})} - 1)\right) \\ = \left(1 + e^{k(P_{\mathrm{PL,m}} - P_{\mathrm{PL,u}})} \frac{\mathrm{TLC_m}}{\mathrm{TLC_u}} + e^{k(P_{\mathrm{PL,l}} - P_{\mathrm{PL,u}})} \frac{\mathrm{TLC_l}}{\mathrm{TLC_u}}\right) V_u \end{aligned} \tag{5.45}$$

Isolating V_u:

$$V_u(t=0) = \frac{V_0 + m\mathrm{TLC_m}\left(e^{k(P_{\mathrm{PL,m}} - P_{\mathrm{PL,u}})} - 1)\right) + m\mathrm{TLC_l}\left(e^{k(P_{\mathrm{PL,l}} - P_{\mathrm{PL,u}})} - 1)\right)}{1 + e^{k(P_{\mathrm{PL,m}} - P_{\mathrm{PL,u}})} \frac{\mathrm{TLC_m}}{\mathrm{TLC_u}} + e^{k(P_{\mathrm{PL,l}} - P_{\mathrm{PL,u}})} \frac{\mathrm{TLC_l}}{\mathrm{TLC_u}}} \tag{5.46}$$

The initial volumens of V_m and V_l are determined with the same precedure and they are detailed in the following equations:

$$V_m(t=0) = \frac{V_0 + m\mathrm{TLC_u}\left(e^{k(P_{\mathrm{PL,u}}-P_{\mathrm{PL,m}})}-1)\right) + m\mathrm{TLC_l}\left(e^{k(P_{\mathrm{PL,l}}-P_{\mathrm{PL,m}})}-1)\right)}{1 + e^{k(P_{\mathrm{PL,u}}-P_{\mathrm{PL,m}})}\dfrac{\mathrm{TLC_u}}{\mathrm{TLC_m}} + e^{k(P_{\mathrm{PL,l}}-P_{\mathrm{PL,m}})}\dfrac{\mathrm{TLC_l}}{\mathrm{TLC_m}}} \tag{5.47}$$

$$V_l(t=0) = \frac{V_0 + m\mathrm{TLC_u}\left(e^{k(P_{\mathrm{PL,u}}-P_{\mathrm{PL,l}})}-1)\right) + m\mathrm{TLC_m}\left(e^{k(P_{\mathrm{PL,m}}-P_{\mathrm{PL,l}})}-1)\right)}{1 + e^{k(P_{\mathrm{PL,u}}-P_{\mathrm{PL,l}})}\dfrac{\mathrm{TLC_u}}{\mathrm{TLC_l}} + e^{k(P_{\mathrm{PL,m}}-P_{\mathrm{PL,l}})}\dfrac{\mathrm{TLC_m}}{\mathrm{TLC_l}}} \tag{5.48}$$

5.5 Choice of values

Once the equations which form the ventilation distribution model have been defined. It is necessary to give values to the different parameters. In the present section, typical values are used and indicated as well as certain parameters, such us the compliances, are determined. This section would be subdivided into three parts:

Anatomical Constants

Typical values for TLC (6.66 liters) and FRC (3.55 liters) are taken from the table 2 of the paper of Salazar and Knowles [SK64] and whose values are a mean of the pressure-volume curve for a group of 20 subjects. The representation of the P-V curve was shown in Fig.5.3.

In order to obtain the values of the lobar total capacities for each lobe $\mathrm{TLC_u}$, $\mathrm{TLC_m}$ and $\mathrm{TLC_l}$, the same anatomical volume assumtions of [WD60] and [BBB$^+$60] have been used. Where 25% of the lung volume is assigned to the upper zone, 36% is assigned to the middle zone and 39% to the lower zone. These values are in compliance with the average results of $\mathrm{TLC_u}$ (45%) and $\mathrm{TLC_l}$ (55%) realized on post mortem human lungs by Pedley et al. [PSME72].

Elastic Constants

The elastic constants are also determined by the P-V curve of [SK64]. The value calculated of m is 1.067, while the value k is 0.0914 [$\mathrm{cmH_2O^{-1}}$]. These values are within the range of values considered realistic [PSME72].

Another values that are calculated in this section are: d_u, d_m and d_l [cm]. The vertical distances between the center of the upper lobe, middle lobe and lower lobe respectively

and the center of the whole lung. The lenght of the lung is the same that the previous chapter (L=23.6 cm). These values are shown in Fig.5.8:

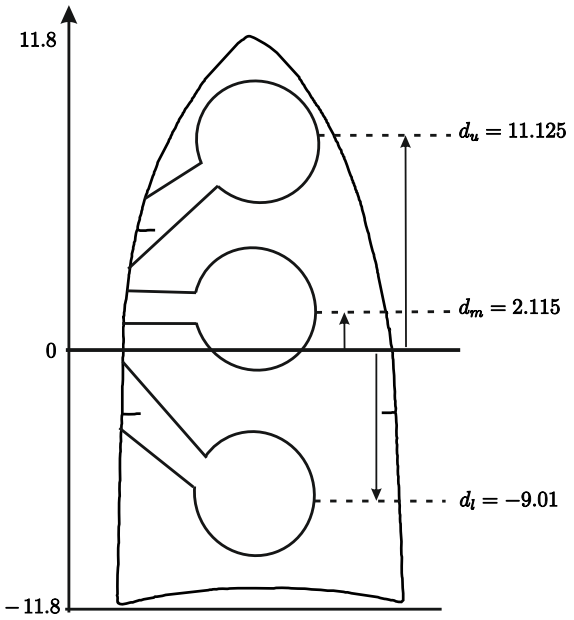

Figure 5.8: Representation of vertical distances between the center of the lung and the centers of the upper, middle and lower lobes

Athought Pedley et al. [PSME72] have determined the centers of the two lobes from the measurements of four post morten humans lungs. The distances values of our model are estimated from the division of the lung in the three zones relized in the previous chapter. The center of each lobe is in the middle of each respective zone. The difference between the center of the lung and the level of the main pulmonary artery and vein is (11.8 cm - 4.3 cm) = 7.5 cm. The distances in the ventilation are calculated as:

$$d_{\mathrm{u}}\,(\text{ventilation}) = d_{\mathrm{u}}\,(\text{perfusion}) - 7.5 = 11.125\text{cm} \tag{5.49a}$$

$$d_{\mathrm{m}}\,(\text{ventilation}) = d_{\mathrm{m}}\,(\text{perfusion}) - 7.5 = 2.125\text{cm} \tag{5.49b}$$

$$d_{\mathrm{l}}\,(\text{ventilation}) = d_{\mathrm{l}}\,(\text{perfusion}) - 7.5 = -9.01\text{cm} \tag{5.49c}$$

Lung Compliances value

Since the inspiration is realized from FRC, when the lung is in equilibrium. The static transpulmonary pressure at the isovolume point, which it depend on the whole lung volume, can be obtained according to the following equation:

$$V_{\mathrm{FRC}} = m\,\mathrm{TLC}\,(1 - e^{-k\,\Delta P_i}) \tag{5.50}$$

Taking the values of $V_{\mathrm{FRC}} = 3.55$ liters, TLC $= 6.66$ liters and $m = 1.067$.

$$1 - \frac{V_{\mathrm{FRC}}}{m\,\mathrm{TLC}} = e^{-k\,\Delta P_i} = 0.5 \tag{5.51}$$

Hence the compliances, using the parameters previously defined, are calculated :

$$C_u = k\,m\,\mathrm{TLC_u}\,(1 - b\,d_u)\,0.5 = 0.0603\ \frac{L}{\mathrm{cmH_2O}} \tag{5.52}$$

$$C_m = k\,m\,\mathrm{TLC_m}\,(1 - b\,d_m)\,0.5 = 0.1110\ \frac{L}{\mathrm{cmH_2O}} \tag{5.53}$$

$$C_l = k\,m\,\mathrm{TLC_l}\,(1 - b\,d_l)\,0.5 = 0.1526\ \frac{L}{\mathrm{cmH_2O}} \tag{5.54}$$

All the parameters described in this Chapter are represented in Tab.5.2:

Table 5.2: Parameters and values ventilation model

Description	Parameter	Value	Units	Localization
Fractional Lung Capacity	V_{FRC}	3.55	L	[SK64]
Total Lung Capacity	TLC	6.66	L	[SK64]
Total Lung Capacity upper lobe	$\mathrm{TLC_u}$	1.665	L	[WD60],[BBB$^+$60]
Total Lung Capacity middle lobe	$\mathrm{TLC_m}$	2.3976	L	[WD60],[BBB$^+$60]
Total Lung Capacity lower lobe	$\mathrm{TLC_l}$	2.5974	L	[WD60],[BBB$^+$60]
Initial Volume upper lobe	$\mathrm{V_u(t=0)}$	1.1145	L	Eq.5.46
Initial Volume middle lobe	$\mathrm{V_m(t=0)}$	1.3395	L	Eq.5.47
Initial Volume lower lobe	$\mathrm{V_l(t=0)}$	1.0960	L	Eq.5.48
Constant	m	1.067	-	[SK64]
Constant	k	0.0914	$\mathrm{cmH_2O^{-1}}$	[SK64]
Constant	b	0.023	$\mathrm{cm^{-1}}$	[MEHD$^+$66][BMEP66]
Airway Resistance	R_{AW}	3	$\mathrm{cmH_2O\,s\,/L}$	[NGV$^+$]
Compliance upper lobe	$\mathrm{C_u}$	0.0603	$\mathrm{L/cmH_2O}$	Eq.5.52
Compliance middle lobe	$\mathrm{C_m}$	0.1110	$\mathrm{L/cmH_2O}$	Eq.5.53
Compliance lower lobe	$\mathrm{C_l}$	0.1526	$\mathrm{L/cmH_2O}$	Eq.5.54
Pleural extended pressure zone 1	$\mathrm{P_{PE,u}}$	16.4671	$\mathrm{cmH_2O}$	Eq.5.1a, Eq.5.18
Pleural extended pressure zone 2	$\mathrm{P_{PE,m}}$	11.0912	$\mathrm{cmH_2O}$	Eq.5.1b, Eq.5.18
Pleural extended pressure zone 3	$\mathrm{P_{PE,l}}$	5.8790	$\mathrm{cmH_2O}$	Eq.5.1c, Eq.5.18
Hydrostatic pressure zone 1	$\mathrm{P_{Hdy,u}}$	-3.2335	$\mathrm{cmH_2O}$	Eq.5.21
Hydrostatic pressure zone 2	$\mathrm{P_{Hdy,m}}$	-0.5456	$\mathrm{cmH_2O}$	Eq.5.22
Hydrostatic pressure zone 3	$\mathrm{P_{Hdy,l}}$	2.0605	$\mathrm{cmH_2O}$	Eq.5.23
Compliance Chest Wall	C_{cw}	0.2	$\mathrm{L/cmH_2O}$	[NGV$^+$]
Dead space Volume	$\mathrm{V_D}$	0.150	L	[GH12]
Distance upper lobe	$\mathrm{d_u}$	11.125	cm	Eq.5.49a
Distance middle lobe	$\mathrm{d_m}$	2.115	cm	Eq.5.49b
Distance lower lobe	$\mathrm{d_l}$	-9.01	cm	Eq.5.49c

6 Simulation and Validation of the Models

The goal of this chapter is to evaluate the results obtained in the simulation of both models. The ventilation model would be analyzed first, then the perfusion model and finally, the ventilation-perfusion rate would be presented and evaluated.

6.1 Ventilation Model

This section focuses on the behavior of ventilation model under spontaneous breathing. The values used in the simulation are taken from Tab.5.2.

6.1.1 Resting position analysis

The following Fig.6.1 represents the different transpulmonary pressures according to the distances of the lung indicated in Tab.5.2. These values are calculated as:

$$P_{\mathrm{TP,u}} = \bar{P}_{\mathrm{ALV}} - (\mathrm{P}_{\mathrm{Hdy,u}} + P_{\mathrm{PL}}) = 0 - (-3.2335 - 5) = 8.2335\mathrm{cmH_2O} \tag{6.1a}$$

$$P_{\mathrm{TP,m}} = \bar{P}_{\mathrm{ALV}} - (\mathrm{P}_{\mathrm{Hdy,m}} + P_{\mathrm{PL}}) = 0 - (-0.5456 - 5) = 5.5456\mathrm{cmH_2O} \tag{6.1b}$$

$$P_{\mathrm{TP,l}} = \bar{P}_{\mathrm{ALV}} - (\mathrm{P}_{\mathrm{Hdy,l}} + P_{\mathrm{PL}}) = 0 - (2.0605 - 5) = 2.9395\mathrm{cmH_2O} \tag{6.1c}$$

$$P_{\mathrm{TP,c}} = \bar{P}_{\mathrm{ALV}} - P_{\mathrm{PL}} = 0 - 5 = 5\mathrm{cmH_2O} \tag{6.1d}$$

Where $P_{\mathrm{TP,c}}$ is the transpulmonary pressure in the center of the lung. The transpulmonary pressure decreases from the top to the bottom of the lung due to the weight of the lung. As a consecuence ,the basal lung in resting position is relatively compressed and it has small resting volumen than the apex, as shown in Fig.6.2. This behavior can be compared with the orientative behavior shown by West [Wes12] and Guyton and Hall [GH12].

As it is shown in Fig.6.1, there is a lineal approximation between the transpulmonary pressure pressure and the distance of the lung. The trampulmonary pressure decrease approximatly 0.263 $\mathrm{cmH_2O}$ per centimeter from the top to the bottom of the lung. The value used in the literature is 0.25 $\mathrm{cmH_2O/cm}$ thus, our value calculated is in accordance with the expected one.

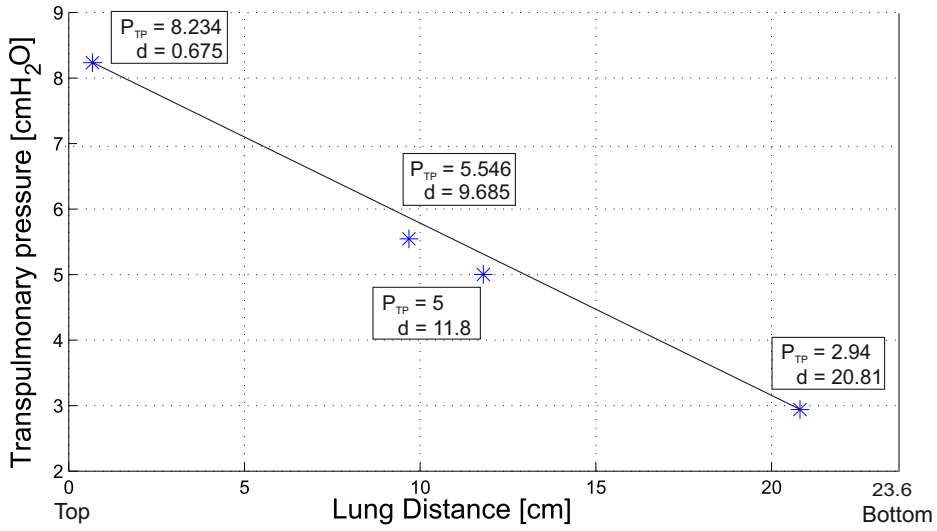

Figure 6.1: Representation of the transpulmonary pressures according to the distance from top of lung at resting position

.

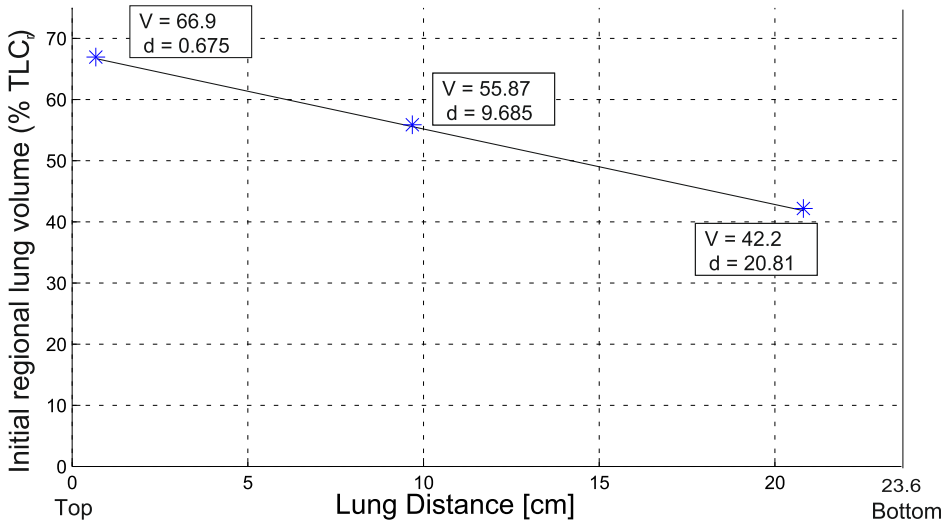

Figure 6.2: Representation of the regional volumen according to the distance from top of the lung at resting position

.

Fig.6.2 represents the initial regional volumen of the three zones at their vertical distances from the apex (see Tab.5.2). The behavior can be compared with Fig.6.3 which contains experimental data of Milic-Emili et al.[MEHD$^+$66], Bryan et al [BMEP66] and Chang et al. [CY99]. This initial regional lung volumens are expressed as percentage of regional lung volume at full inspiration :

$$\frac{V_u(t=0)}{\mathrm{TLC_u}} * 100 = 66.9 \tag{6.2a}$$

$$\frac{V_m(t=0)}{\mathrm{TLC_m}} * 100 = 55.8 \tag{6.2b}$$

$$\frac{V_l(t=0)}{\mathrm{TLC_l}} * 100 = 42.2 \tag{6.2c}$$

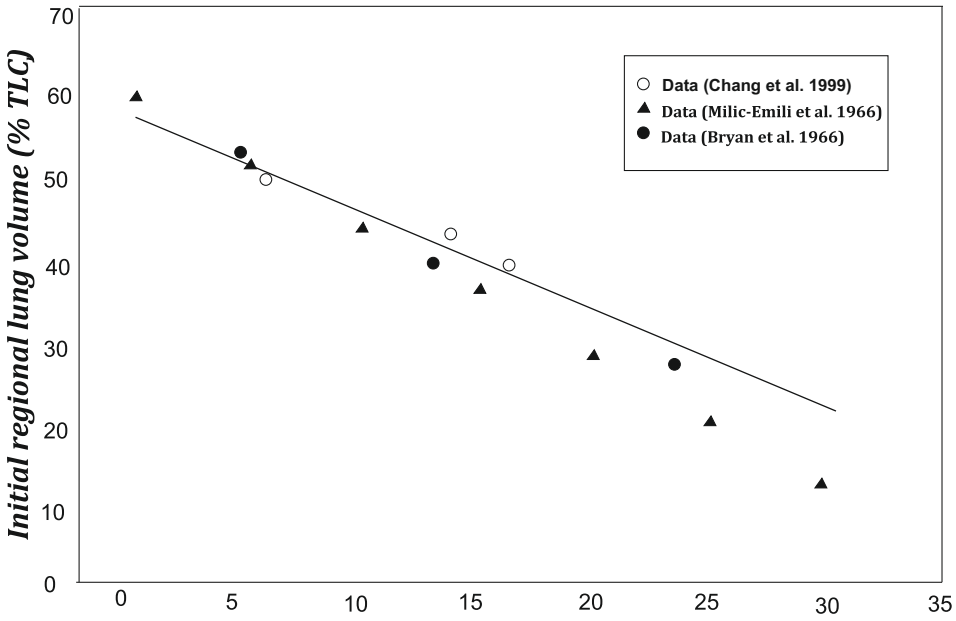

Figure 6.3: Initial Regional lung volume %TLC$_\mathrm{r}$ according to vertical distance from the apex of the lung (cm) of Bryan et al. [BMEP66], Milic-Emili et al. [MEHD$^+$66] and [CY99]. Adapted from [CY99]

We can calculate in our simulation (Fig.6.2) the percentage of volume that decreases per centimeter, it is 1.2267 %/cm. On the other hand, the percetage of volume that decrease per centimeter in Fig.6.3 is calculated from the mean of the data of the authors and its value is 1.2 %/cm approximately. Therefore, our results are in good agreement with the literature.

6.1.2 Dynamic behavior of the lung

In this subsection, the behavior of the lung would be analysed during the inspiration and expiration. The following Fig.6.4 represents the changes of alveolar pressure (P_{ALV}), pleural pressure (P_{PL}) and thus transpulmonary pressure (P_{TP}) during spontaneuos breathing in the three lobes and the whole lung. All of these variables are simulated during 150 seconds. However, Fig.6.4 and Fig.6.5 only represent the interval of time between 80 and 90 seconds (10 seconds).

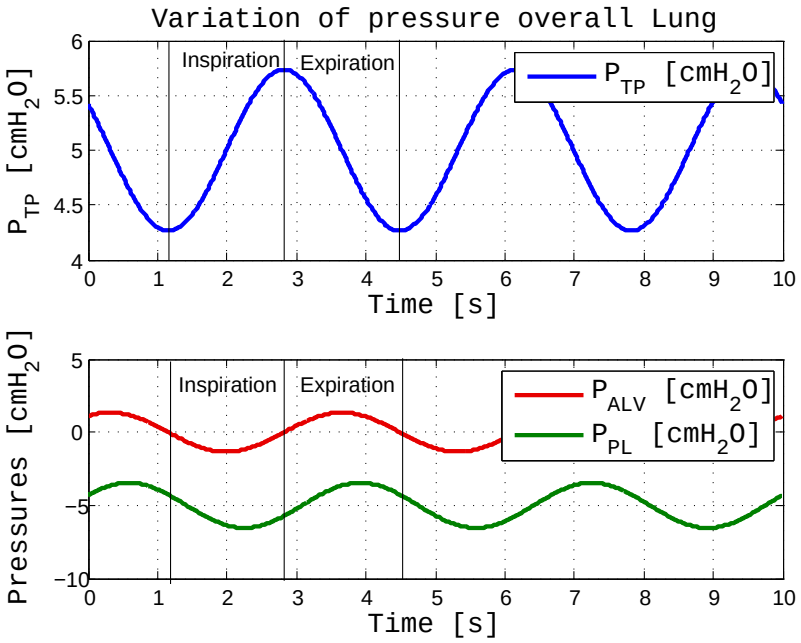

Figure 6.4: Alveolar, Pleural and Transpulmonary pressures overall lung

.

The simulation (Fig.6.4) shows a decrese of alveolar pressure during the inspiration. The volume of the thoracic cavity increases and as a result of this thorax expansion, the pleural (or intrapleural pressure) also decreases. A detailed explication is decrited in Chap.2. On the other hand, the transpulmonary pressure which is the difference between both pressures increases. During expiration, the alveolar pressure rises as is shown in the simulation. Besides the thorax is contracted and the intrapleural pressure also increases. In this case, the transpulmonary pressure is reduced.

The Fig.6.5 represents this changes of transpulmonary pressures in the three zones of the lung. As it is seen, the traspulmonary pressure is greater in the top of the lung than in the base during all time, as it is expected. It is due to the different intrapleural pressures in the zones, because the alveolar pressure keeps the same wave form in the three lobes.

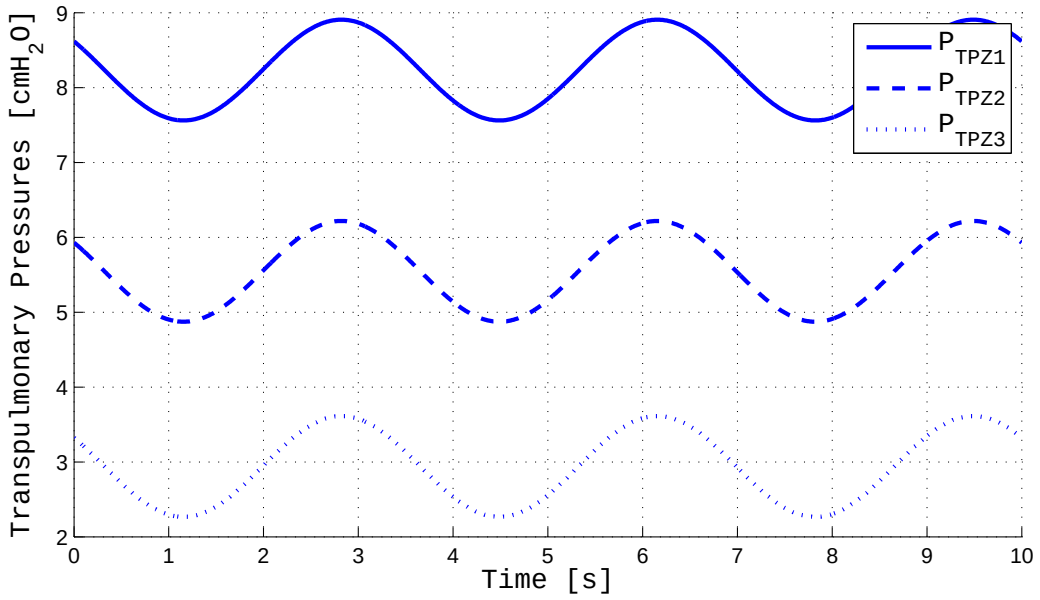

Figure 6.5: Variation of transpulmonary pressures in the three lobes during spontaneous breathing

As a result of the inspiration the volume of the lung increses while it decreases during expiration. Fig 6.6 represents a relationship bethween the overall volume and the volume of the diverse zones during the respiration. Whilst the Fig.6.7 shows the ventilation (L/s) in the whole lung and in the three zones.

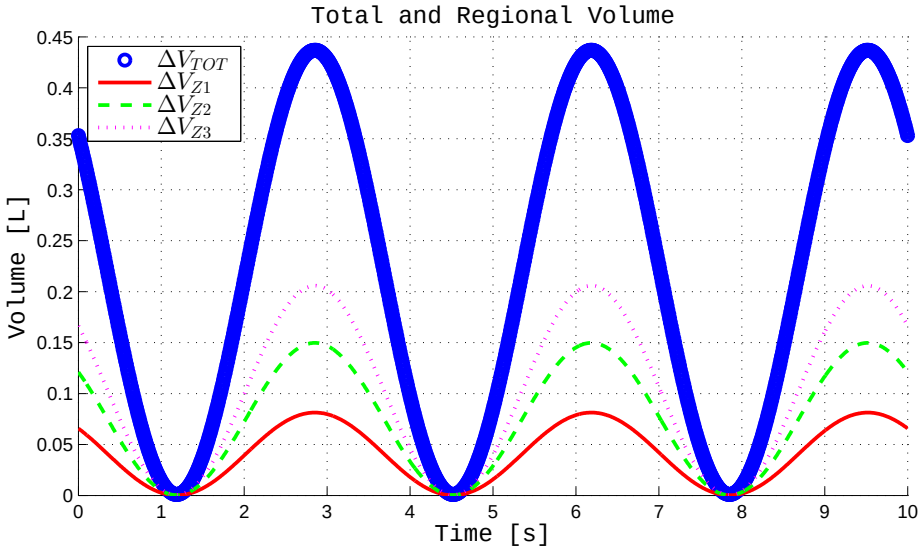

Figure 6.6: Variation of volumes in the overall lung, zone 1, zone 2 and zone 3 during spontaneous breathing

.

Fig.6.6 represents the change on volumes from the volume at resting position (FRC). It is

indicated in the graph as volume equal to zero. During inspiration the volumens start to inscrease until the end of the inspiration (tidal volumen ,V_T). After that, the expiration begins and the volumes decrease until the rate of change equal to zero. As it is shown in the Fig.6.6, the sum of the regional volume in each zone is equal to the overall lung volume, as it is expected. Moreover, the regional volume in the zone 3 is greater than the remaining regional volumes as it it shown in Fig.6.6. It is because of the basal lung expands more on inspiration than the middle region and the apex, therefore it has a larger change on volume. The same explication can be used for the difference of change on volume between the zone 2 and zone 1.

As the change on volume is greater in zone 3, the ventilation must be larger that the others zones. Moreover, the overall ventilation is also equal to the sum of the regional ventilations which it is the expected. This behavior of the lung is shown in Fig.6.7.

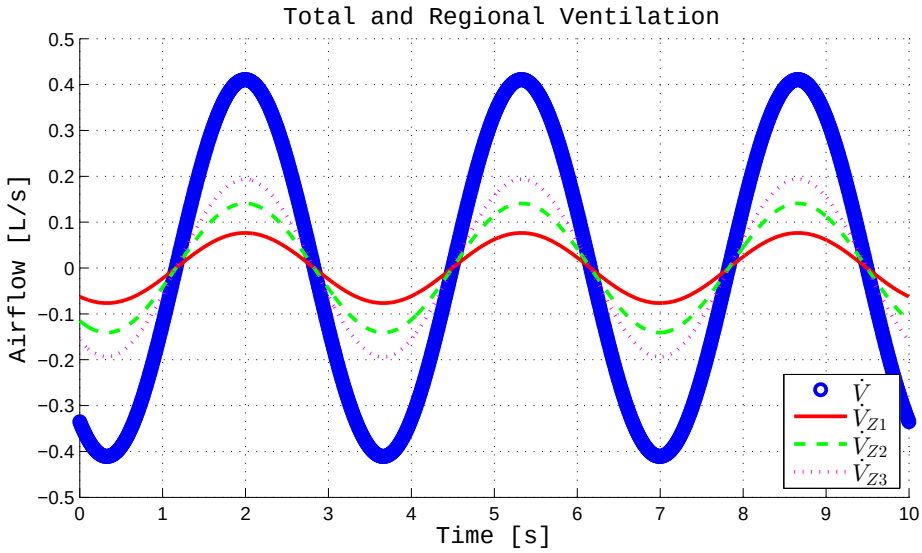

Figure 6.7: Variation of ventilation in the overall lung, zone 1, zone 2 and zone 3 during spontaneous breathing

.

Fig.6.8 correspond to the simulations between the changes on volumen and transpulmonary pressure during normal breathing in the three lobes of the lung. Comparing them, the variantion in the three transpulmonary pressure is approximatly the same. It is around 1.5 (cmH_2O) between the pressure at resting position and the end of inspiration. On the other hand, it has more effect on volume in the lower zone (zone 3) than in the middle (zone 2) and upper zones (zone 1) due to the expansion of the lung as it was explained before.

An importan phenomenon known as **hyteresis** is presented in the following three P-V curves. The hysteresis appears because there is a marked difference in the pressure change at the same volume, both inflation and deflation. The ascending part ,indicated with an arrow in the graphic, applies to inflation and the descending part to deflation.

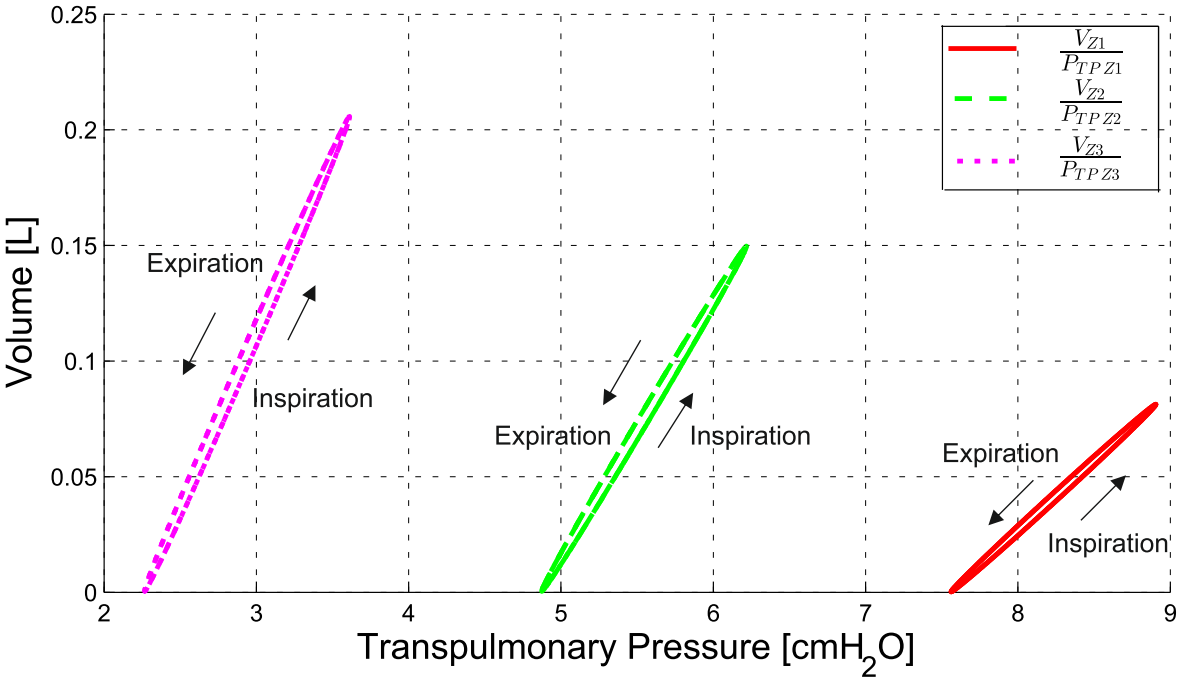

Figure 6.8: Pressure-Volume curves in the three zones during spontaneous breathing

.

6.2 Perfusion Model

In this section we analyze the behavior of our perfusion model. In this analysis, differents variables such as pressure, flow, the relashionship between them has been considered. The Tab.6.1 shows the parameters used to the simulations.

Table 6.1: Parameters and values perfusion model

Description	Parameter	Value	Units	Localization
Arterial Resistance zone 1	$R_{a,u}$	100000	$cmH_2O\,s\,/L$	-
Capillar Resistance zone 1	$R_{c,u}$	100000	$cmH_2O\,s\,/L$	-
Venous Resistance zone 1	$R_{v,u}$	100000	$cmH_2O\,s\,/L$	-
Capillary bed Compliance zone 1	$C_{cp,u}$	0.351	L/cmH_2O	Eq.6.3b
Arterial Resistance zone 2	$R_{a,m}$	184.1796	$cmH_2O\,s\,/L$	Eq.4.17
Capillar Resistance zone 2	$R_{c,m}$	106.0428	$cmH_2O\,s\,/L$	Eq.4.17
Arterial Resistance zone 3	$R_{a,l}$	148.8346	$cmH_2O\,s\,/L$	Eq.4.15
Capillar Resistance zone 3	$R_{c,l}$	24.8058	$cmH_2O\,s\,/L$	Eq.4.15
Venous Resistance zone 3	$R_{v,l}$	11.6259	$cmH_2O\,s\,/L$	Eq.4.15
Capillary bed Compliance zone 3	$C_{cp,l}$	0.351	L/cmH_2O	Eq.6.3b
Hydrostatic pressure zone 1	$P_{Hdy,u}$	19.7492	cmH_2O	Eq.4.10b
Hydrostatic pressure zone 2	$P_{Hdy,m}$	10.1954	cmH_2O	Eq.4.11b
Hydrostatic pressure zone 3	$P_{Hdy,l}$	-1.6011	cmH_2O	Eq.4.12b

The arterial, capillary and venous resistance in the zone 1 emulate infinites resistance (see Sec.4.2) thus, we have chosen a high value: 100000 $cmH_2O\,s\,/L$ for each resistance. The value of the capillary bed compliance in the zone 1 and zone 2 are the same. Linehan et al. [LDR82] and Rippe et al. [RPT+87] determinated that the capillary compliance corresponds to 75% of the total compliance. The total compliance is the sum of the pulmonary artery compliance, pulmonary venous compliance and pulmonary capillary bed compliance. The values of the pulmonary artery and venous comliance are taken from [BP11](C_{pa}=0.1149 L/cmH_2O and C_{pv}=0.0022 L/cmH_2O). As a result:

$$C_T = \sum C_{pa} + C_{cp} + C_{pv} \tag{6.3a}$$

$$C_{cp} = 0.75 * C_T = \frac{0.75 * (C_{pa} + C_{pv})}{1 - 0.75} = 0.351\,L/cmH_2O \tag{6.3b}$$

6.2.1 Static behavior

In this subsection we would analyse the perfusion of the lung when the pulmonary artery pressure (P_{pa}), the pulmonary vein pressure (P_{pv}) and the alveolar pressure (P_{ALV}) are in average. The mean used are 19.033 cmH_2O (14 mmHg) [BP11], 1.359 cmH_2O (1 mmHg)[BP11] and 0 cmH_2O respectively [GH12]. The results of the simulations would be compared with the data from West [WDN64] in order to test the behavior of our lung. The values of blood flow respresented in our simulation corresponds to the data from West [WD60](see Sec:4.2, Sec:4.4, Sec:4.3):

Table 6.2: Blood flow upper,middle and lower zones

Description	Parameter	Value
Blood flow zone 1	q_u	0 L/s
Blood flow zone 2	q_m	1.9 L/min = 0.0317 L/s
Blood flow zone 3	q_l	3.4 L/min = 0.0567 L/s

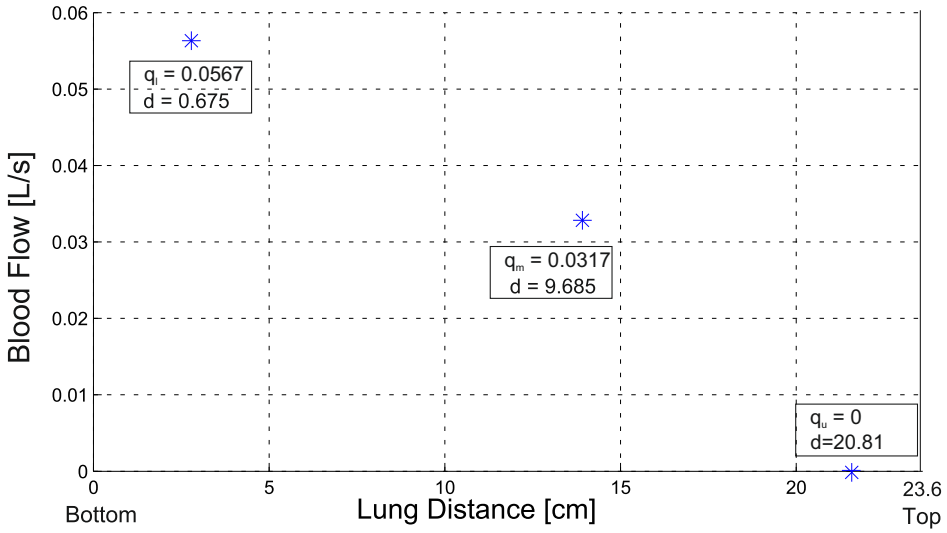

Figure 6.9: Blood flow distribution in the lung

Fig.6.10 represents the increment of blood flow per unit volume with distance down the isolated perfused upright dog lung. Above the point at which the pulmonary artery pressure is equal to alveolar pressure, there is no blood flow. As it seen in the results of our model Fig 6.9, the behavior is quite similar to the one obtained by West. Blood flow increases with the distance down the lung and the blood flow in the top of the lung is zero because the alveolar pressure exceeds the pulmonary artery pressure. (P_{ALV} = 0 cmH_2O, P_{pa} = 19.033 - $P_{Hdy,l}$ cmH_2O).

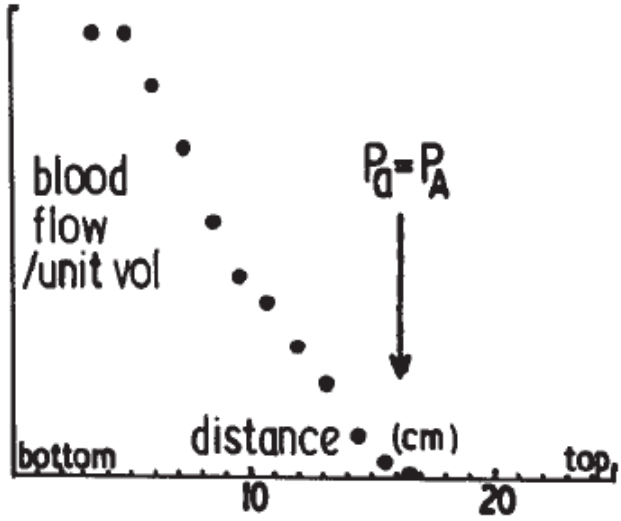

Figure 6.10: Blood flow distribution by West [WDN64] along the lung of dog

6.2.2 Dynamic behavior heart

In this section we evaluate the flow throughout the lung in the three zones during the beating of the heart. Therefore the pulmonary artery and venous pressure change during systole and diastole and thereby the blood flow. The following simulations show the changes of blood flow in the three zones of the lung during the interval of time between 80 and 90 seconds (10 seconds).

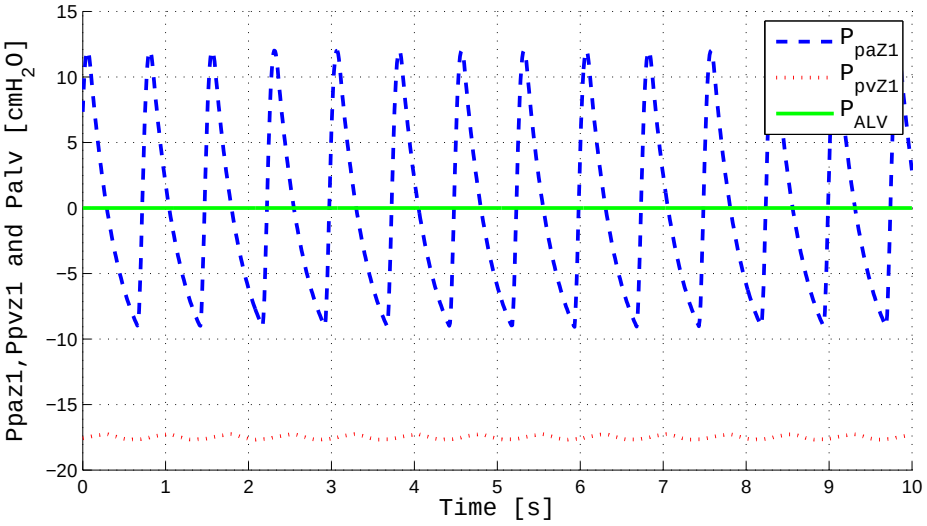

Figure 6.11: Pulmonary artery pressure, pulmonary venous pressure and alveolar pressure during heart beats zone 1

As it is seen in the simulation Fig.6.11, the pulmonary artery pressure is greater than the alveolar pressure during systole in zone 1 when the pulmonary artery pressure is greater than 19.033 cmH_2O. Although the blood flows in these instants of time, in our model we have assumed that the blood does not flow in the first zone of the lung. Therefore, the blood flow represented in the simulation Fig.6.12 is approximately zero.

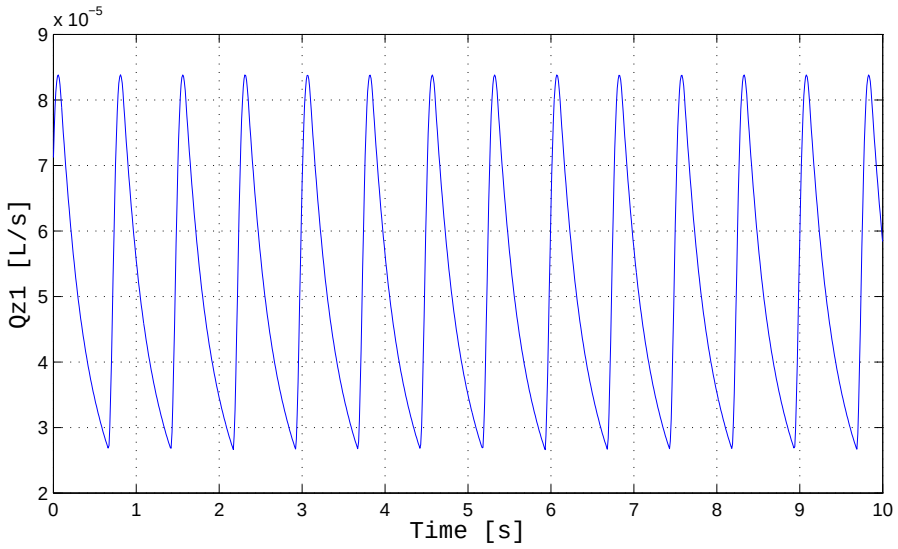

Figure 6.12: Dynamic blood flow distribution zone 1

.

Fig.6.12 shows the blood flow in zone 1 of the lung. The values fluctuate between $3 * 10^{-5}$ and $9 * 10^{-5}$ L/s. Therefore, the behavior is the expected. On the other hand, Fig.6.14 represents the blood flow in the zone 2 of the lung. In this case the perfusion varies between 0 and 0.08 L/s, whose mean is 0.0328 L/s. It is slightly higher than expected (0.0317 L/s). Finally, the Fig.6.16 shown the variation of blood flow in the zone 3 of the lung. As it is seen, their values are greater than the zone 2. The perfusion fluctuates between 0.03 and 0.1 L/s and its mean is 0.0563 L/s. In this case, the mean is approximatly the expected (0.0567 L/s). It should be pointed that these means have been calculated between the 80 and 90 seconds when the system is stable.

As we indicated in Sec.4.4 the pulmonary arterial pressure is greater than the alveolar pressure, but the alveolar pressure is greater than the pulmonary venous pressure in zone 2. The simulation Fig.6.13 shows this difference of pressures. Moreover, during systole the pulmonary artery and venous pressure increase while during diastole both pressures decrease. This variation produces the blood flow fluctuates as shows Fig.6.14.

On the other hand, as we indicated in Sec.4.3 the pulmonary arterial and venous pressure are greater than the alveolar pressure in zone 3. The simulation Fig.6.15 shows this difference of pressures. Moreover, the blood flow variation is represented in Fig.6.16.

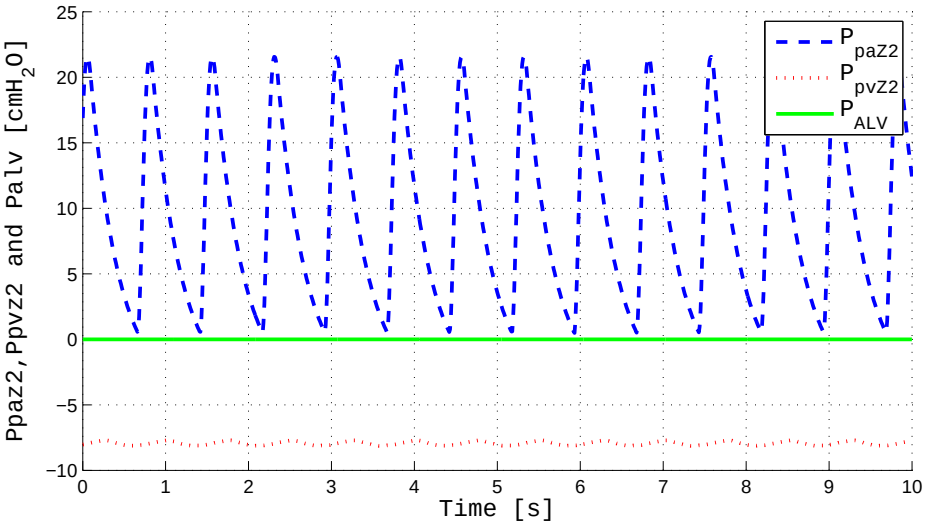

Figure 6.13: Pulmonary artery pressure, pulmonary venous pressure and alveolar pressure during heart beats zone 2

.

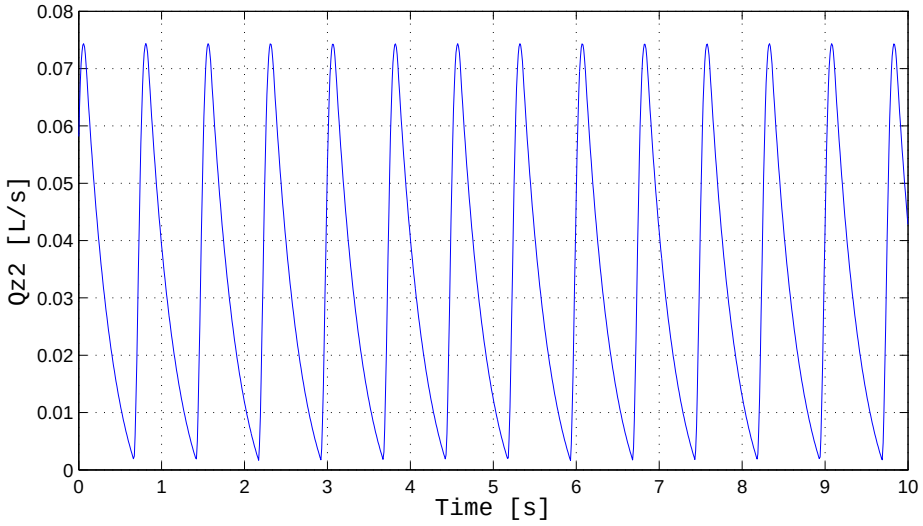

Figure 6.14: Dynamic blood flow distribution zone 2

.

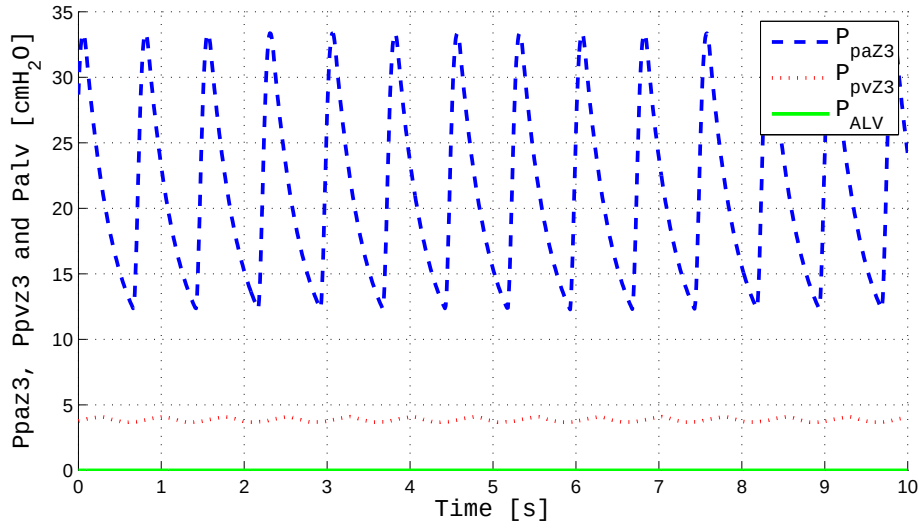

Figure 6.15: Pulmonary artery pressure, pulmonary venous pressure and alveolar pressure during heart beats zone 3

.

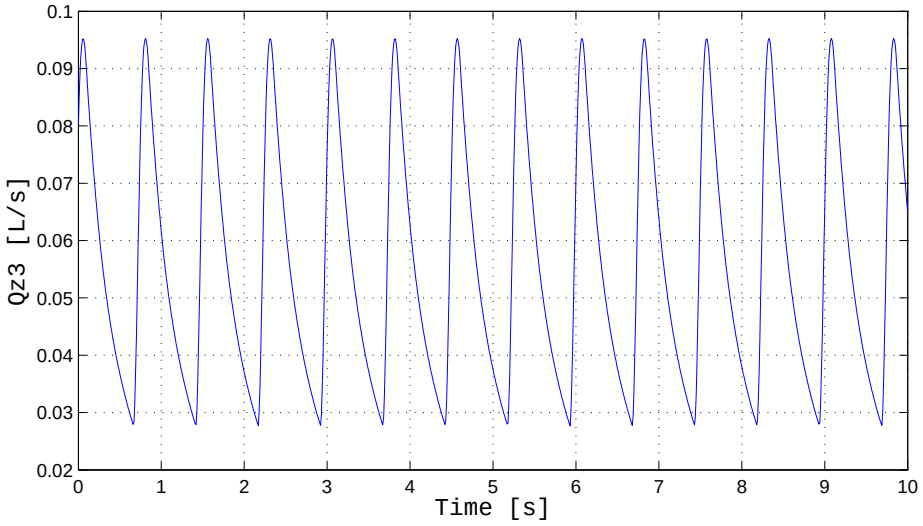

Figure 6.16: Dynamic blood flow distribution zone 3

.

6.3 Ventilation-Perfusion Closed Loop

In this section, it is presented the simulations and results when we combine the ventilation and the perfusion model. We would evaluate the ventilation-perfusion rate as well as the effect of the ventilation in the perfusion.

The simulations Fig.6.18, Fig.6.20 and Fig.6.22 show the oscillation in the blood flows waveform in the three zones of the lung. This is because of the variation in the thoracic pressure (pelural pressure) during spontaneos breathing in the perfusion. As it is seen in Fig.6.17, Fig.6.19 and Fig.6.21 during spontaneos breathing the pulmonary artery and venous pressure fluctuate with the same frecuency than the pleural pressure, 0.3 Hz. As a result, the blood flows of the three zones varie with this same frecuency. It should be noted that the three blood flow signals keep approximately the same blood flow mean as it is shown in Tab.6.5. In addition, it should be pointed that these means have been calculated between the 80 and 90 seconds when the system is stable.

In simulations Fig.6.17, Fig.6.19 and Fig.6.21 are represented the pulmonary artery, venous and alveolar pressures in zone 1, zone 2 and zone 3, respectively. As it is seen, these simulations have the characteristic that we described in Sec.4.3, Sec.4.4 and Sec.4.3, respectively.

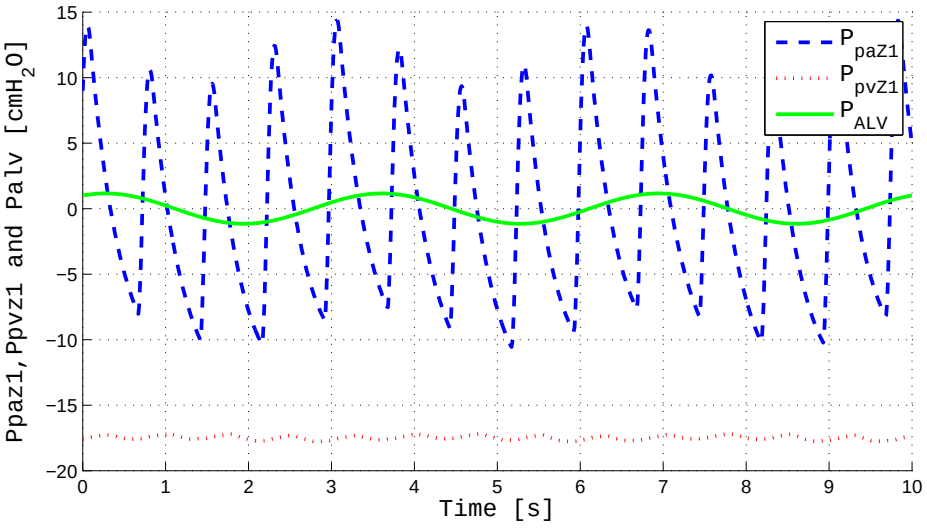

Figure 6.17: Pulmonary artery pressure, pulmonary venous pressure and alveolar pressure during heart beats and ventilation zone 1

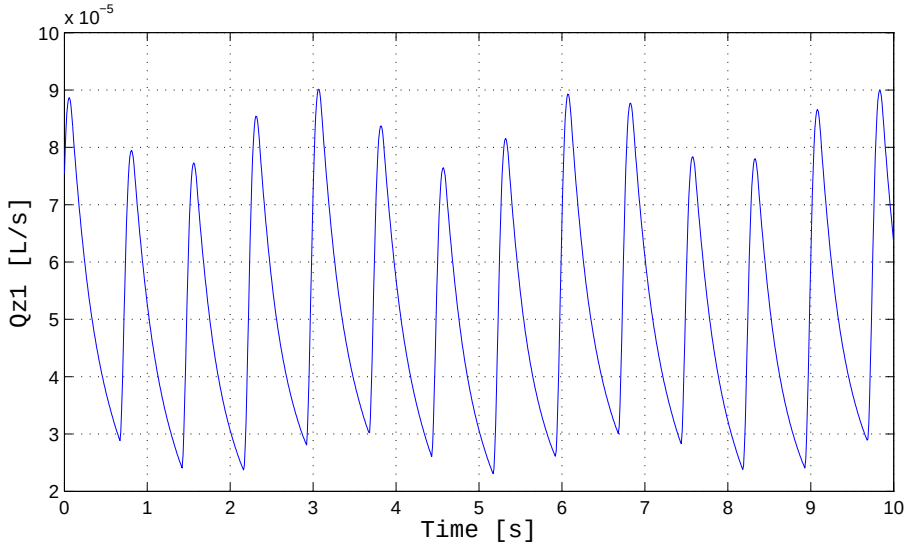

Figure 6.18: Dynamic blood flow distribution zone 1 with ventilation

.

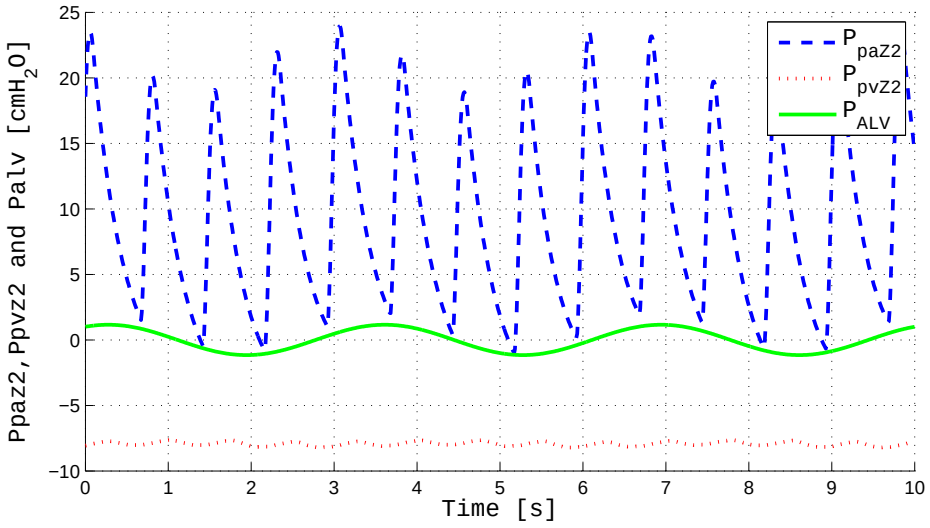

Figure 6.19: Pulmonary artery pressure, pulmonary venous pressure and alveolar pressure during heart beats and ventilation zone 2

.

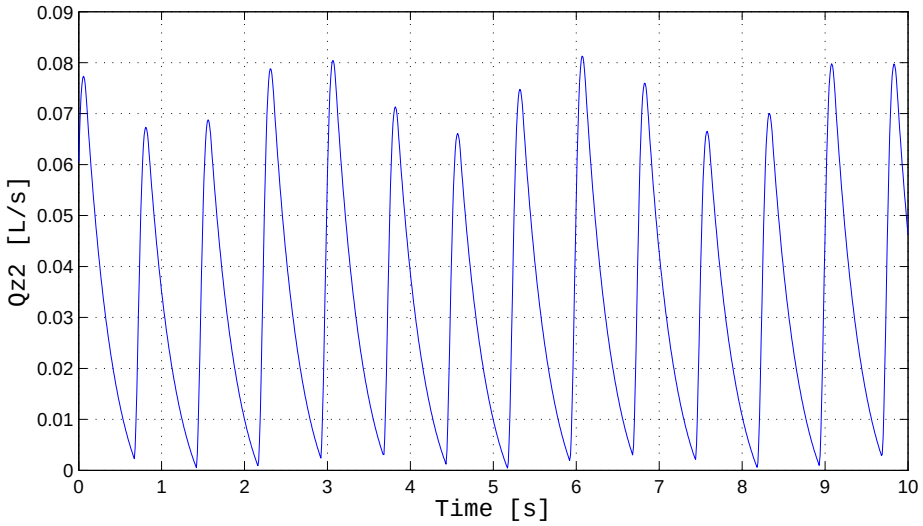

Figure 6.20: Dynamic blood flow distribution zone 2 with ventilation

.

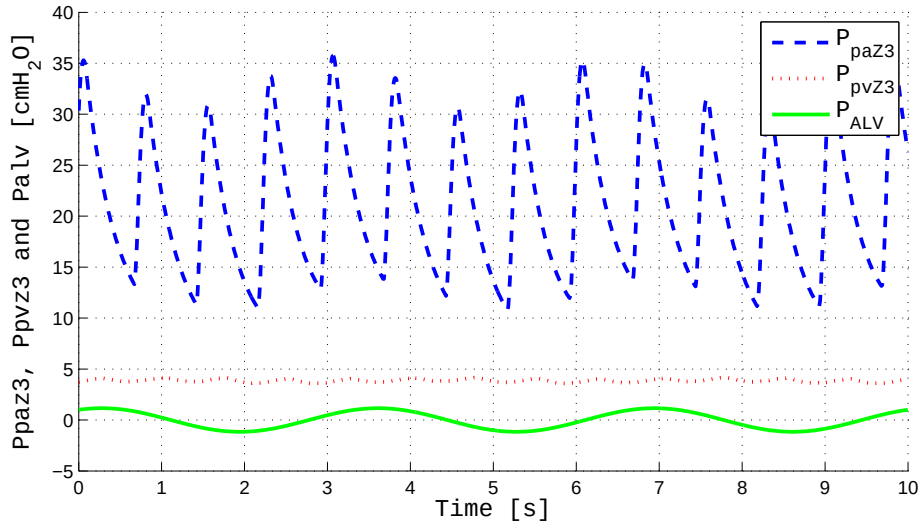

Figure 6.21: Pulmonary artery pressure, pulmonary venous pressure and alveolar pressure during heart beats and ventilation zone 3

.

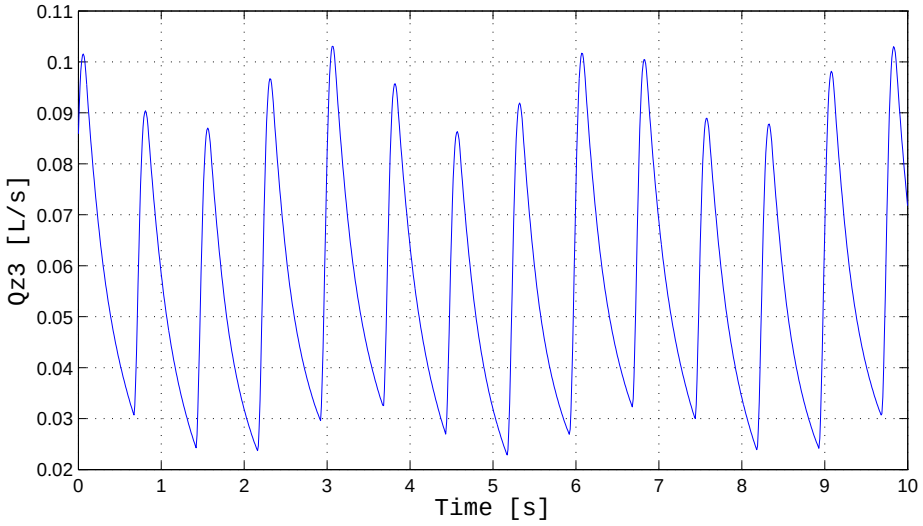

Figure 6.22: Dynamic blood flow distribution zone 3 with ventilation

.

In order to calculate the ventilation perfusion rate, it is necessary to obtain the alveolar ventilation in the whole lung and in each zone of the lung as well as the mean blood flow in the same zones. The values are indicated in Tab.6.4 and Tab.6.5 respectively.

Table 6.3: Resulting blood flow mean in the whole lung and in each zone

Description	Value	Units
Blood flow overall lung	0.0887	L /s
Blood flow zone 1	4.3509e-05	L /s
Blood flow zone 2	0.0326	L /s
Blood flow zone 3	0.0561	L /s

Table 6.4: Resulting alveolar ventilation in the whole lung and in each lobe

Description	Value	Units
Alveolar ventilation overall lung	0.0861	L /s
Alveolar ventilation zone 1	0.0160	L /s
Alveolar ventilation zone 2	0.0295	L /s
Alveolar ventilation zone 3	0.0405	L /s

The resulting ventilation-perfusion rates are calculated dividing the alveolar ventilation and the mean blood flow. The value are shown in Tab.6.5. Comparing our results with

the data of the table 1 of West and Dollery [WD60] , our overall ventilation-perfusion rate is greater 0.97 with respect 0.848 of West. That is because of we have not considered blood flow in the upper zone of the lung whilst West and Dollery [WD60] obtained slightly blood flow in that region in their analisys. As a result the values represented in Tab.6.5 are slightly greater.

However, the overall behaviour of the lung is as expected. The zone 1 is characterized by being a ventilated but unperfused area. Therefore, the ventilation-perfusion rate must be higher as it is show in Tab.6.5. On the other hand, zone 3 is charazterized by being a perfused but no ventilated area, as a result, the ventilatilation-perfusion rate must be lower. In this case, our ventilation-perfusion rate in that zone is slightly greater. The zone 2 is characterized by have the same proportion in ventilation than perfusion, thus our ventilation-perfusion rate is according with the expected. In general we can conclude that our models represents a correct behavior of the lung.

Table 6.5: Ventilation-perfusion rate

Description	Value
Ventilation-perfusion rate overall lung	0.97
Ventilation-perfusion rate zone 1	367.74
Ventilation-perfusion rate zone 2	0.9049
Ventilation-perfusion rate zone 3	0.7219

7 Conclusions and Future work

This chapter contains a conclusion of the thesis. The second part gives different utilities and aspect that could be developed to improve the models.

7.1 Conclusions

During the development of this thesis, the goal has been to create a perfusion-distribution model and a ventilation-distribution model in order to model the ventilation-perfusion mismatch along the lung. Althouth diverse physiological componets such as the viscosity of the blood and the geometry of the alveoli have influence in the ventilation and in the perfusion, in both models we focus on the effects of gravity.

The lung is divided in three zones, the upper zone (zone 1), the middle zone (zone 2) and the lower zone (zone 3) in order to describe the effects of gravity on pulmonary capillary blood flow and on the transpulmonary pressure. To model the perfusion we have considered the pressure-flow relationships along the lung whilst to model the ventilation, the pressure-volume relationship has been treated. As a result, we accomplish a complete model of perfusion and ventilation which presents a good representation of the lung.

At resting position the upper lobe of the lung are more expanded than the middle and lower lobes. As a result, ventilation during spontaneous breathing was found nonuniform with more air entering in the lower lobes than the middle and upper lobes. The experimental results obtained with the ventilation distribution model simulation in Sec.6.1 show its stability and ability to simulate accurately the behavior expected. This results are also compared with the literature [CY99] and [MEHD$^+$66] to verify the correct operation of our model. On the other hand, the gravity produce an increment of intravascular pressure resulting in more recruitment and distension of vessels, as a result the resistance to blood decreases and consequently, the blood flow increases. The perfusion distribution model represents this behavior depicted in the simulations in Sec.6.2. Moreover, this results have been compare with the data obtained by West et al. [WDN64] to validate our model.

Finally the different ventilation-perfusion rate obtained in each zone are compared with the data provided by West and Dollery [WD60]. The results obtained in the simulations are in good agreement with the results of the literature. Therefore, we can certificate that the behavior of both models is as expected.

7.2 Future work

- Since both models have been developed under an upright position, these can be improved to simulate the lungs in supine position and in different ranges of inclination in order to evaluate their effects in the regions of the lung.

- Besides the models can be completed by including more zones i.e fourth zones where the zone 4 located on the bottom of the lung is characterized by ARDS recruitment in order to analysed it and to represent more faithfully the physiology of the lung.

- On the other hand, the slow breathing and ventilation machine model previously developed can be included in our ventilation model in future works and test its influence in the ventilation and perfusion models.

- Moreover the gas-exchange model can be include in the future in order to evaluate the gas-exchange at different regions of the lung

A Appendix

A.1 Perfusion Model

A.1.1 Upper Model

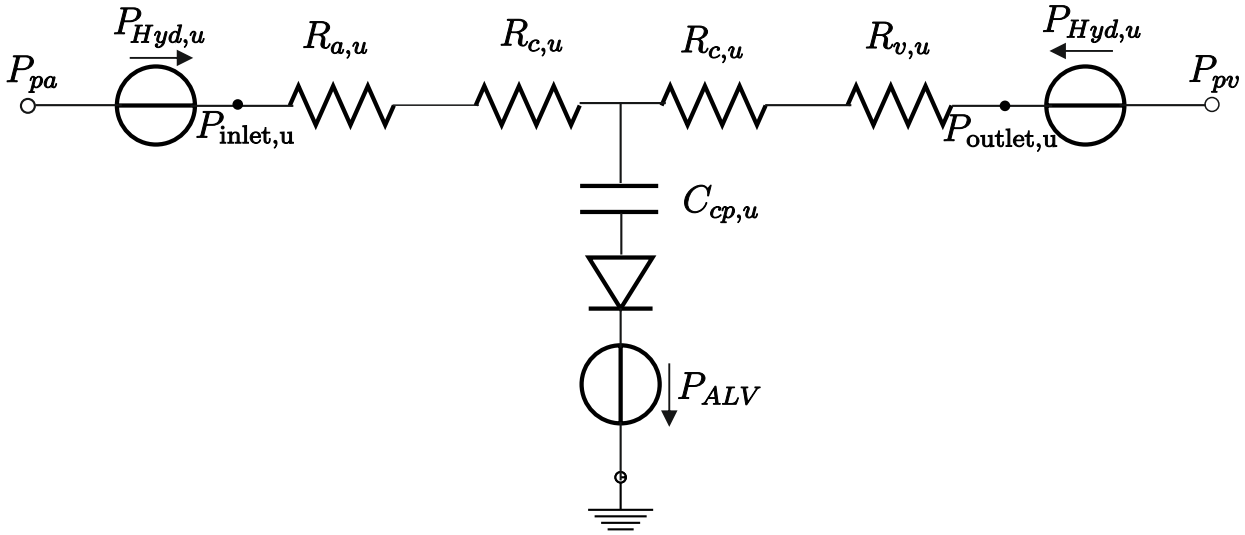

Figure A.1: Circuit model that represent the zone 1

.

A.1.2 Middle Model

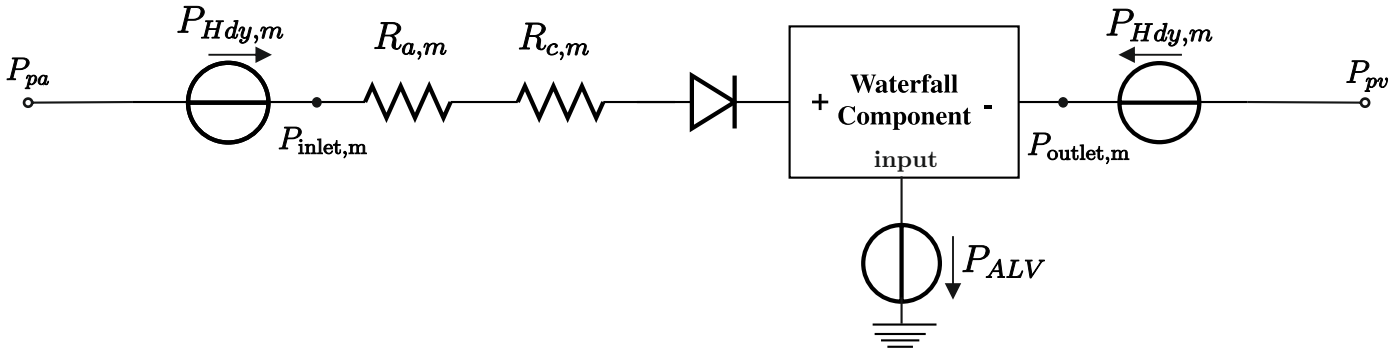

Figure A.2: Circuit model Waterfall effect (zone 2)

.

A.1.3 Lower Model

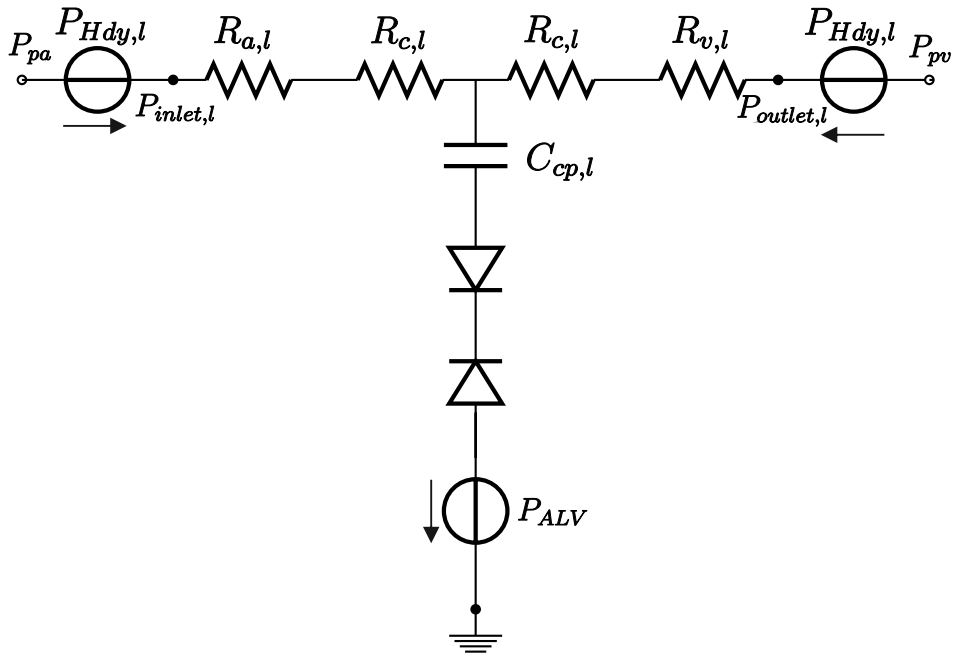

Figure A.3: Circuit model that represent the zone 3

A.1.4 Complete Perfusion Model

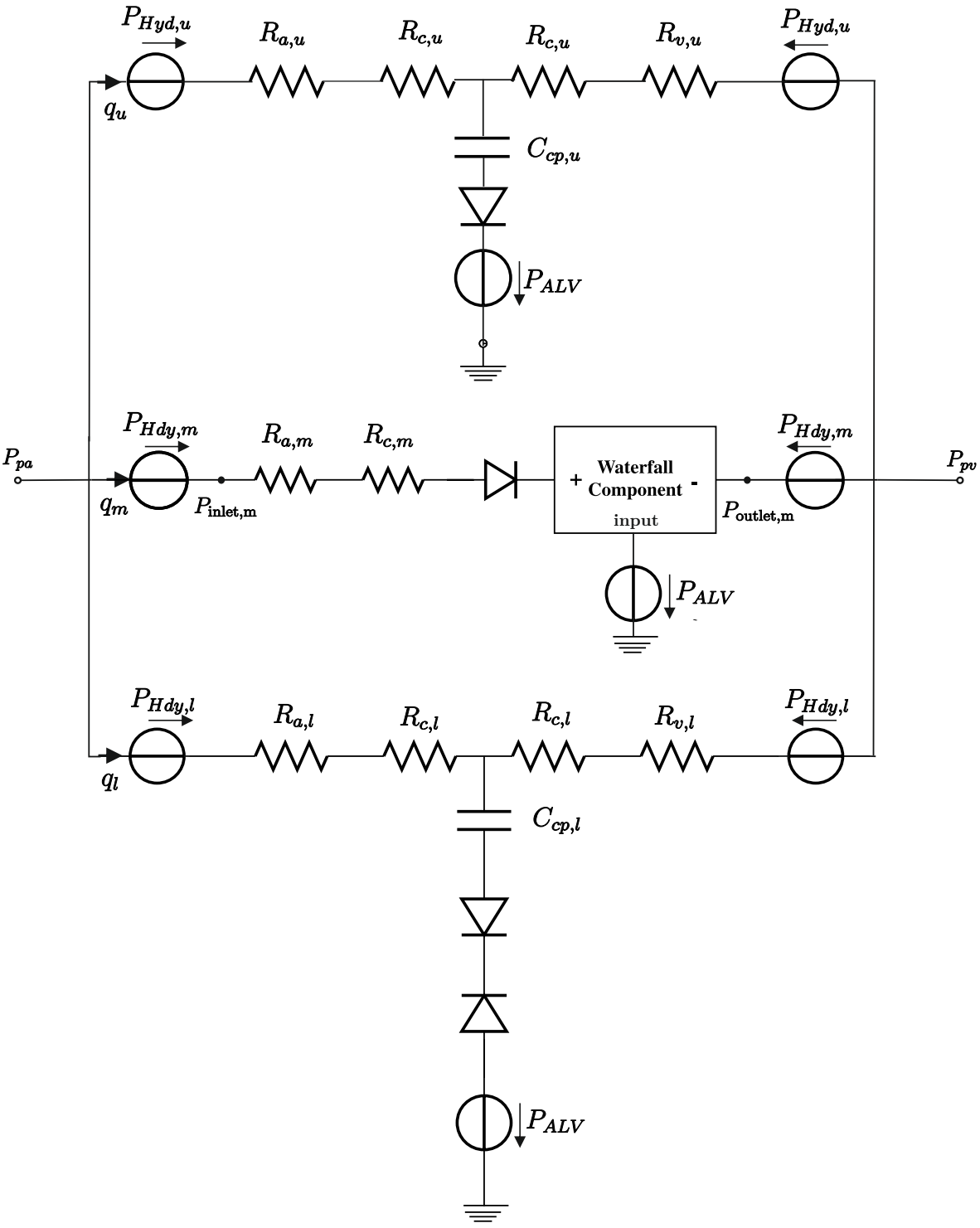

Figure A.4: Circuit model that represent the three zones

.

A.2 Ventilation Model

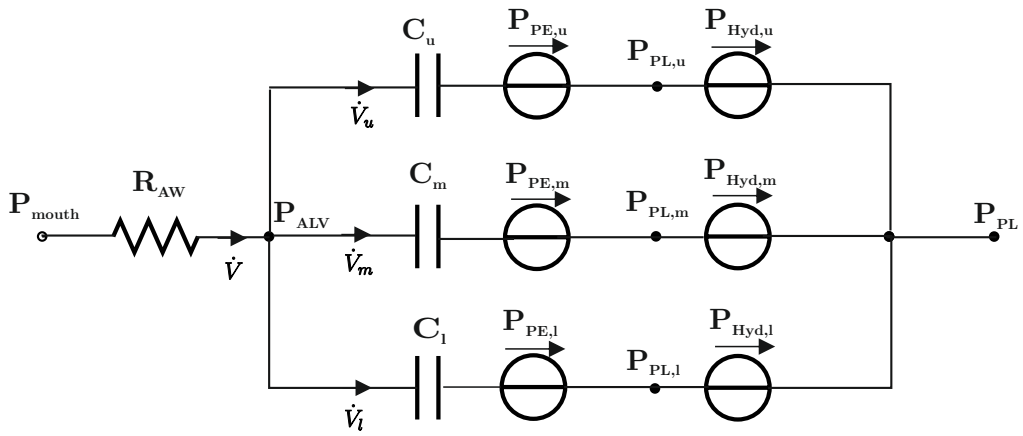

Figure A.5: Electrical circuit equivalent to the ventilation distribution model developed

.

A.3 Heart

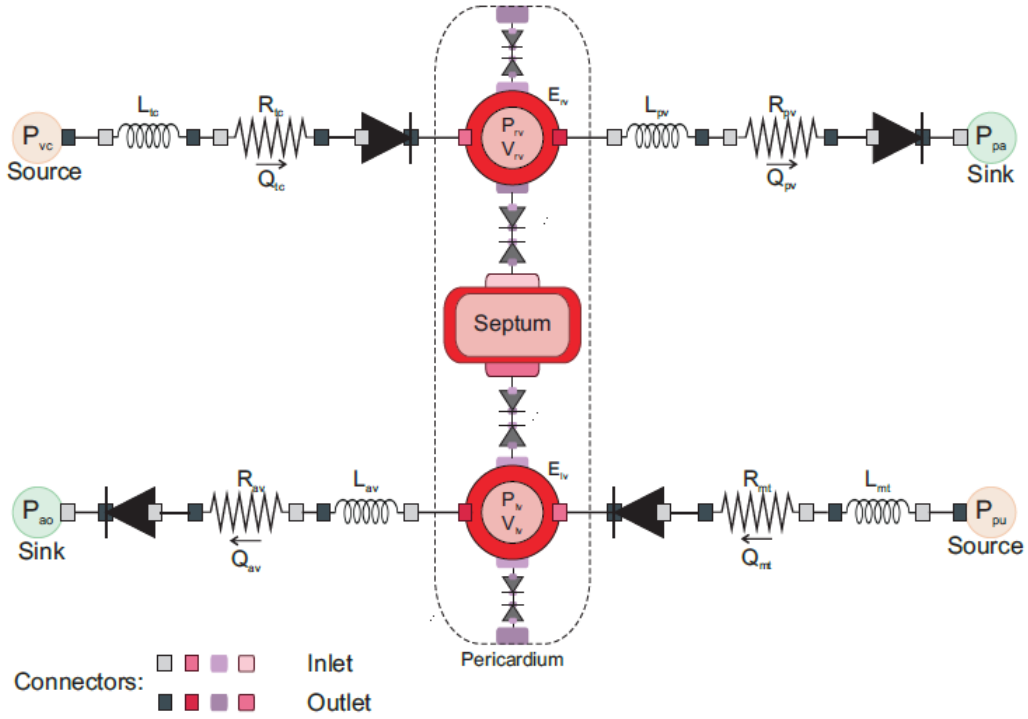

Figure A.6: Heart

.

A.4 Lung

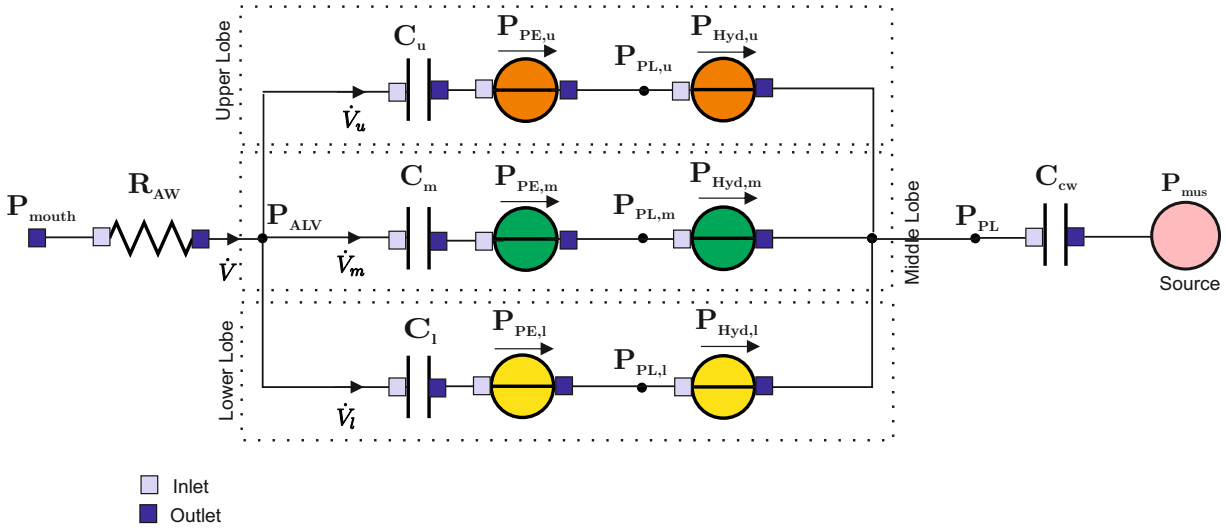

Figure A.7: Lung

.

A.5 Closed Loop Model

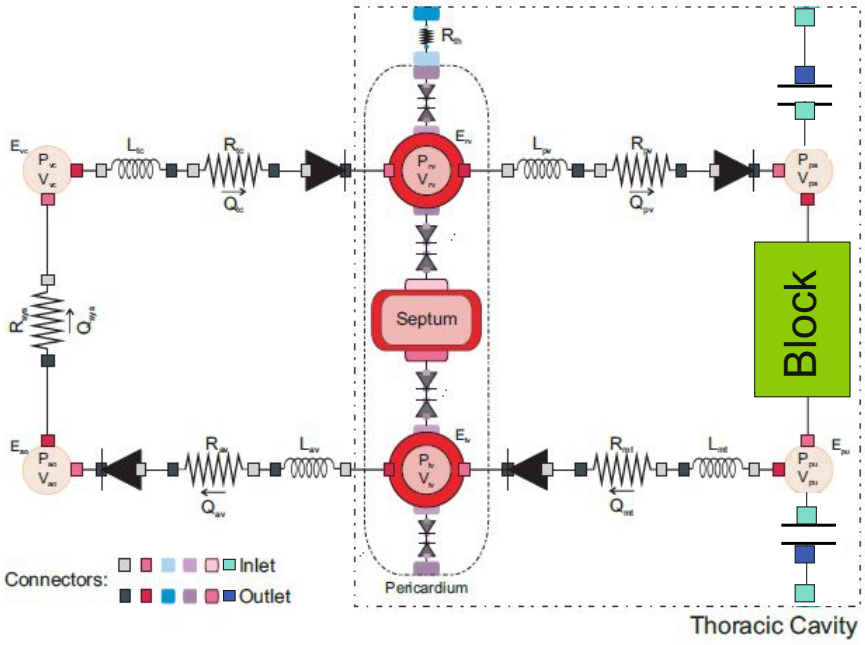

Figure A.8: Closed Loop Model

.

Block

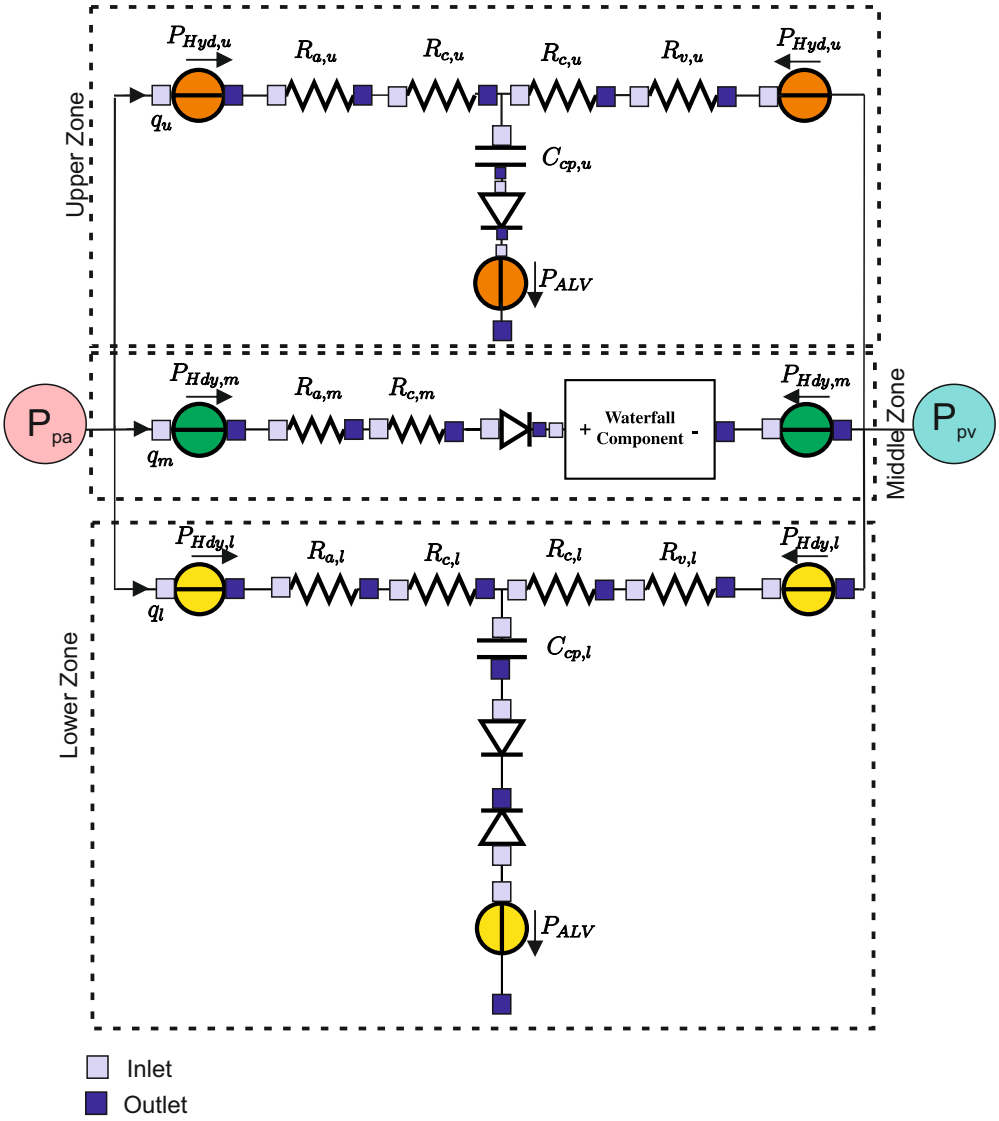

Figure A.9: Lung Perfusion

.

Bibliography

[Bat09] Bates, Jason H. T.: *Lung Mechanics: An Inverse Modeling Approach*. New York : Cambridge University press, 2009

[BBB+60] Bryan, A. C. ; Bentivoglio, L. G. ; Beerel, F. ; Macleish, H. ; Zidulka, A. ; Bates, D. V.: Factors affecting regional distribution of ventilation and perfusion in the lung. In: *Journal of Applied Physiology* 15 (1960), S. 405–410

[BMEP66] Bryan, A.C. ; Milic-Emili, J. ; Pengelly, D.: Effect of Gravity on the Distribution of Pulmonary Ventilation. In: *Journal of Applied Physiology* 21 (1966), S. 778–784

[BP11] Barbosa Pereira, Carina: *Modelling the (Failing) Human Heart in the Objected Oriented Modellig Language Dymola*, Lehrstuhl fÃ¼r medizinische informationstechnik (mediT), Diss., August 2011

[BSD68] Brody, J. S. ; Stemmler, E. J. ; DuBois, A. B.: Longitudinal distribution of vascular resistance in the pulmonary arteries, capillaries and veins. In: *The Journal of Clinical Investigation* 47 (1968), S. 783–799

[BT06] Ben-Tal, A.: Simplified models for gas exchange in the human lungs. In: *Journal of Theoretical Biology* 238 (2006), S. 474–495

[CY99] Chang, Y. H. ; Yu, C. P.: A model of ventilation disrtibution in the human lung. In: *Aerosol Science and Technology* 9 (1999), S. 309–319

[DGL77] Dawson, C. A. ; Grimm, D. J. ; Linehan, J. H.: Effect of lung inflation on longitudinal distribution of pulmonary vascular resistance. In: *Journal of Applied Physiology* 43 (1977), S. 1089–1092

[DK75] Downey, H.F. ; Kirk, E. S.: Inhibition of coronary blood flow by a vascular waterfall mechanism. In: *Circulation Research* 36 (1975), S. 753–760

[FIR] *Forum of International Respiratory Societies*. `http://www.firsnet.org/`,

[GH12] Guyton, Arthur C. ; Hall, Jhon E.: *Textbook of Medical Physiology*. 11. Elsevier Saunders, 2012

[Gle08] Glenny, R. W.: Teaching ventilation/perfusion relationships in the lung. In: *Advances in Physiology Education* 32 (2008), S. 192–195

[GTOG67] Gaar, K. A. J. ; Taylor, A. E. ; Owens, L. T. ; Guyton, A. C.: Pulmonary capillary pressure and filtration coefficient in the isolated perfused lung. In: *Journal of Applied Physiology* 213 (1967), S. 910–914

[Hel04] Heldt, Thomas: *Computational Models of Cardiovascular Response to Orthostatic Stress*, Harvard - MIT Division of Health Sciences and Technology, Diss., September 2004

[Hla72] Hlastala, M.P.: A model of fluctuating alveolar gas exchange during the respiratory cycle. In: *Respiration Physiology* 15 (1972), S. 214–232

[HMC82] Hakim, T. S. ; Michel, R. P. ; Chang, H. K.: Partitioning of pulmonary vascular resistance in dogs by arterial and venous occlusion. In: *Journal of Applied Physiology* 52 (1982), S. 710–715

[KKA+10] Karbing, D. S. ; Kjaergaars, S. ; Andreassen, S. ; Espersen, K. ; Rees, S. E.: Minimal model quantification of pulmonary gas exchange in intensive care patients. In: *Medical Engineering and Physics* (2010)

[LC73] Lin, K.H. ; Cumming, G: A model of time-varying gas exchange in the human lung during a respiratory cycle at rest. In: *Respiration Physiology* 17 (1973), S. 93–112

[LC78] Lewis, Milena L. ; Christianson, Lynn C.: Behavior of the human pulmonary circulation during head-up tilt. In: *Journal of Applied Physiology* 45(2) (1978), S. 249–254

[LDR82] Linehan, J. H. ; Dawson, C. A. ; Rickaby, D. A.: Distribution of vascular resistance and compliance in a dog lung lobe. In: *Journal of Applied Physiology* 53 (1982), S. 158–168

[LNCJ+98] Liu, C. H. ; Niranjan, S. C. ; Clark Jr., J. W. ; San, K. Y. ; Zwischenberger, J. B. ; Bidani, A.: Airway mechanics, gas exchange , and blood flow in a nonlinear model of the normal human lung. In: *Journal of Applied Physiology* 84 (1998), S. 1447–1469

[LWHR82] Lambert, R. K. ; Wilson, T. A. ; Hyatt, R. E. ; Rodarte, J. R.: A computational model for expiration flow. In: *Journal of Applied Physiology* 52 (1982), S. 44–56

[MAT] *MATLAB SIMULINK and SIMSCAPE (2015).* `http://de.mathworks.com/`,

[Mea61] Mead, J.: Mechanical properties of lungs. In: *Physiological Reviews* 41 (1961), S. 281–330

[MEHD+66] Milic-Emili, J. ; Henderson, J. A. M. ; Dolovich, M. B. ; Trop, D. ; Kaneko, K.: Regional distribution of inspired gas in the lung. In: *Journal of Applied Physiology* 21 (1966), S. 749–759

[Mog11] Mogensen, Mads L.: *A physiological mathematical model of the respiratory system*, Departament of Health Science and Technology. Alborg University, Diss., 2011

[MSKA09] Mogensen, M. L. ; Steimle, K. L. ; Karbing, D. S. ; Andreassen, S.: A mathematical physiological model of the pulmonary capillary perfusion. In: *Departament of Health Science and Technology, Aalborg University, Denmark* (2009)

[MY56] Martin, C. J. ; Young, A. C.: Lobar ventilation in man. In: *American Review of Tuberculosis* 73 (1956), S. 330–337

[NGV+] Ngo, Chuong ; Gerno, Misgeld ; Vollmer, Thomas ; Winter, Stefan ; Leonhardt, Steffen: Linear affine lung mechanics model with emphasis on pleural dynamics. In: *Chair of Medical Information Technology, Helmholz Institut for Biomedical Engineering, RWTH Aachen University*

[OMB+56] Otis, Arthur B. ; McKerrow, Colin B. ; Bartlett, Jere Richard A. an M. Richard A. an Mead ; Mcllroy, M. B. ; Selverstone, N. J. ; Radford JR, E. P.: Mechanical Factors in Distribution of Pulmonary Ventilation. In: *Journal of Applied Physiology* 8 (1956), S. 427–443

[PC] *Pulmonary Circulation.* `http://www.mananatomy.com/wp-content/uploads/2011/04/pulmonary_circulation.jpg`,

[PSME72] Pedley, T. J. ; Sudlow, M. F. ; Milic-Emili, J.: A non-linear theory of the distribution of pulmonary ventilation. In: *Respiration Physiology* 15 (1972), S. 1–38

[Res] *The Respiratory System.* `http://www.nhlbi.nih.gov/health/health-topics/topics/hlw/system/`,

[RPT+87] Rippe, B. ; Parker, J. C. ; Townsley, M. I. ; Mortillaro, N. A. ; Taylor, A. E.: Segmental vascular resistances and compliances in dog lung. In: *Journal of Applied Physiology* 62 (1987), S. 1206–1215

[SK64] Salazar, E. ; Knowles, J. H.: An Analysis of Pressure-Volume Characteristics of the Lungs. In: *Journal of Applied Physiology* 19 (1964), S. 97–104

[SKME68] Sutherland, P. W. ; Katsura, T. ; Milic-Emili, J.: Previous Volume

History of the Lung and Regional Distribution of Gas. In: *Journal of Applied Physiology* 25 (1968), S. 566–574

[WD60] West, J. B. ; Dollery, C. T.: Distribution of blood flow and ventilation-perfusion ratio in the lung, measured with radioactive CO_2. In: *Journal of Applied Physiology* 15 (1960), S. 405–410

[WD13] West, J. B. ; Dollery, C. T.: Fragility of pulmonary capillaries. In: *Journal of Applied Physiology* 115 (2013), S. 1–15

[WDN64] West, J. B. ; Dollery, C. T. ; Naimark, A: Distribution of blood flow in isolated lung; relation to vascular and alveolar pressures. In: *Journal of Applied Physiology* 19 (1964), S. 713–724

[Wes12] West, John B.: *Respiratory Physiology: The Essentials*. 9. Lippincott Williams and Wilkins, 2012

[YS80] Yeh, J. B. ; Schum, G. M.: Models of Human Lung Airways and Their Application to Inhaled Particle Deposition. In: *Bulletin of Mathematical Biology* 42 (1980), S. 461–480